Aus dem Institut für Virologie
der Universität zu Köln
Direktor: Universitätsprofessor Dr. med. F. Klein

Evaluation of scFvs based on HIV-1 Broadly Neutralizing Antibodies as a potential Binding Domain of CAR T Cells

Inaugural-Dissertation zur Erlangung der Doktorwürde
der Medizinischen Fakultät
der Universität zu Köln

vorgelegt von
Franziska Bach
aus Engelskirchen

promoviert am 01. Oktober 2024

Gedruckt mit Genehmigung der Medizinischen Fakultät der Universität zu Köln

2024

Dekan: Universitätsprofessor Dr. med. G. R. Fink

1. Gutachter: Professor Dr. med. F. Klein

2. Gutachterin: Universitätsprofessorin PhD C. Niessen

Erklärung

Ich erkläre hiermit, dass ich die vorliegende Dissertationsschrift ohne unzulässige Hilfe Dritter und ohne Benutzung anderer als der angegebenen Hilfsmittel angefertigt habe; die aus fremden Quellen direkt oder indirekt übernommenen Gedanken sind als solche kenntlich gemacht.

Bei der Auswahl und Auswertung des Materials sowie bei der Herstellung des Manuskriptes habe ich Unterstützungsleistungen von folgenden Personen:

Professor Dr. med. F. Klein
Dr. med. Henning Grüll

Weitere Personen waren an der Erstellung der vorliegenden Arbeit nicht beteiligt. Insbesondere habe ich nicht die Hilfe einer Promotionsberaterin/eines Promotionsberaters in Anspruch genommen. Dritte haben von mir weder unmittelbar noch mittelbar geldwerte Leistungen für Arbeiten erhalten, die im Zusammenhang mit dem Inhalt der vorgelegten Dissertationsschrift stehen.

Die Dissertationsschrift wurde von mir bisher weder im Inland noch im Ausland in gleicher oder ähnlicher Form einer anderen Prüfungsbehörde vorgelegt.

Die in dieser Arbeit angegebenen Experimente sind nach entsprechender Anleitung durch Herrn Professor Dr. med. Florian Klein und Dr. med. Herrn Henning Grüll und von mir selbst ausgeführt worden. Zudem sind die dieser Arbeit zugrunde liegenden Experimente von mir mit Unterstützung von Frau Hanna Janicki einer medizinisch-technischen Assistentin durchgeführt worden.

Die Experimente/ Humanisierung der Versuchstiere wurden gemeinsam mit Frau Dr. rer. med. Daniela Weiland, Herr Dr. med. Henning Grüll und Frau Carola Ruping durchgeführt. Die FACS Analyse wurde von mir selbstständig durchgeführt.

Erklärung zur guten wissenschaftlichen Praxis:

Ich erkläre hiermit, dass ich die Ordnung zur Sicherung guter wissenschaftlicher Praxis und zum Umgang mit wissenschaftlichem Fehlverhalten (Amtliche Mitteilung der Universität zu Köln AM 132/2020) der Universität zu Köln gelesen habe und verpflichte mich hiermit, die dort genannten Vorgaben bei allen wissenschaftlichen Tätigkeiten zu beachten und umzusetzen.

Köln, den 11. Dezember 2024

Unterschrift: F.Bach

Danksagung

An dieser Stelle möchte ich mich bei all denjenigen bedanken, die mich während der Anfertigung dieser Doktorarbeit unterstützt haben. Insbesondere gilt mein Dank den folgenden Personen, ohne deren Hilfe die Anfertigung dieser Doktorarbeit niemals zustande gekommen wären: Mein Dank gilt zunächst meinem Doktorvater, Herrn Prof. Dr. Florian Klein, für die Betreuung dieser Arbeit, sowie der freundlichen Hilfe und Unterstützung. Insbesondere der konstruktive Austausch und die regelmäßigen Gespräche auf fachlicher und persönlicher Ebene waren stets eine große Hilfe für mich und haben mich stets positiv beeinflusst und ermutigt. Zudem gilt mein besonderer Dank Dr. Henning Grüll, der mich mit viel Zeit und Geduld in die Welt des wissenschaftlichen Arbeitens eingeführt hat und immer ein offenes Ohr für Fragen hatte. Darüber hinaus möchte ich Dr. Daniela Weiland, Hanna Janicki, Dr. Meryem Seda Ercanoglu, Carola Ruping, Dr. Christoph Kreer und Dr. Maria Guschlbauer danken, die mich in jeglicher Hinsicht unterstützt haben und die Zeit unvergesslich gemacht haben.

Meinen Eltern danke ich für ihre Geduld und Unterstützung während des gesamten Studiums und der Arbeit an dieser Dissertation.

Zum Schluss möchte ich meinen Freunden und vor allem Oliver Koster herzlich danken für die aufmerksame, liebevolle und vielseitige Unterstützung während des Verfassens dieser Arbeit.

Table of Contents

LIST OF ABBREVIATIONS 6

1. SUMMARY 7

2. ZUSAMMENFASSUNG 9

3. INTRODUCTION 11

3.1 Human Immunodeficiency Virus (HIV) 11
3.1.1. Epidemiology 11
3.1.2. Transmission 12
3.1.3. HIV Envelope Protein 13
3.1.4. Antiretroviral Therapy 14

3.2 Broadly Neutralizing Antibodies (bNAbs) 14
3.2.1. Characteristics of bNAbs 15
3.2.2. Clinical Application of bNAbs 16

3.3 CAR T Cells 17
3.3.1. T Cell Receptor/CD3 Complex 17
3.3.2. Design of CARs 18
3.3.3. Ectodomain 18
3.3.4. Endodomain 18
3.3.5. Anti-HIV-1-CAR 20
3.3.6. Need for Control of CAR T Cell Therapy 20

3.4 Use of small animal models in HIV research 21

3.5 Aims, Objectives and Hypothesis of the Thesis 22

4. MATERIALS AND METHODS 23

4.1 Materials 23

4.2 Methods 26
4.2.1. Mouse Models 26
4.2.2. Cell Lines 26
4.2.3. Cloning of scFv and Full-length Antibody Plasmids 26
4.2.4. Antibody Production and Purification 28

4.2.5. HIV-1 Envelope Protein Production 28
4.2.6. HIV-1-Env ELISA 28
4.2.7. Cell Surface Binding 29
4.2.8. Half-Life Determination in Non-Humanized Mice 29
4.2.9. HEp-2 Cell Immunofluorescence Assay 30
4.2.10. Neutralization Assay 30
4.2.11. Humanization of NOD-Rag1^{null}IL2rg^{null} (NRG) Mice 31
4.2.12. Statistical Analysis 32

5. RESULTS 33

5.1 Generation of Plasmid Constructs and Antibody Production 33

5.2 HIV-1 Envelope Protein Production 37

5.3 HIV-1-Env ELISA 38

5.4 Cell Surface Binding 39

5.5 Half-Life Determination in Non-Humanized Mice 41

5.6 HEp-2 Cell Immunofluorescence Assay 43

5.7 Antibody Neutralization Assay 46

5.8 Humanization of NOD-Rag1^{null}IL2rg^{null} Mice 48

6. DISCUSSION 50

6.1 Essential Properties of IgG1 Antibodies are retained as scFvs 50

6.2 Extended Half-Life of scFv *in vivo* and Establishment of a Humanized Mouse Model 52

6.3 scFvs as a suitable Candidate for the Target Domain 53

7. CONCLUSION 55

8. REFERENCES 56

9. APPENDIX 65

9.1 List of Figures 65

9.2 List of Tables 65

List of Abbreviations

ACT	Adoptive Cell Therapy
AIDS	Acquired Immunodeficiency Ayndrome
ALL	Acute Lymphoblastic Leukemia
ART	Antiretroviral Therapy
bnAb	Broadly Neutralizing Antibody
BSA	Bovine Serum Albumin
CAR	Chimeric Antigen Receptor
CD4	Cluster of differentiation 4
CD3	Cluster of differentiation 3
CD8	Cluster of differentiation 8
CD19	Cluster of differentiation 19
CD28	Cluster of differentiation 28
CDR3	Complementarity Determining Region 3
CRS	Cytotoxic Release Syndrome
CTL	Cytotoxic T Lymphocytes
CCR5	C-C Chemokine Receptor Type 5
CXCR4	C-X-C Chemokine Receptor Type 4
EGFR	Epidermal Growth Factor Receptor
ELISA	Enzyme Linked Immunosorbent Assay
Env	Envelope Protein
FACS	Fluorescence-activated Cell Scanning
FBS	Fetal Bovine Serum
Fc	Fragment crystallizable
FcR	Fc Receptor
FDA	Food and Drug Administration
FITC	Fluorescein Isothiocyanate
GFP	Green Fluorescent Protein
gp140	Glycoprotein 140
gp160	Glycoprotein 160
HBS	HEPES Buffered Saline
HCDR3	Heavy Chain Complementarity-Determining Region 3
HEp-2	Human Epithelial
HIV	Human Immunodeficiency Virus
HLA	Human Leukocyte Antigen
HRP	Horseradish Peroxidase
HSC	Hematopoietic Stem Cells
HTLV	Human T-lymphotropic Retrovirus
IFN-γ	Interferon-γ
IgG1	Immunoglobulin G 1
IgG4	Immunoglobulin G 4
IL-1	Interleukin-1
IL-2	Interleukin-2
IL-6	Interleukin-6
LRA	Latency Reversing Agents
MFI	Mean/ Median Fluorescence Intensity
MHC	Major Histocompatibility Complex
MPER	Membrane Proximal External Region
MSM	Men who have sex with Men
MuLV	Murine Leukemia Virus
NOD	Non-obese diabetic
NRG	NOD-Rag-gamma
PCR	Polymerase Chain Reaction
PBS	Phosphate-buffered Saline
PEI	Polyethylenimine
Rag1^{null}	Recombinase Activating Gene 1
scFv	Single Chain Variable Fragment
SIV	Simian Immunodeficiency Virus
SPF	Specific Pathogen Free
TCR	T Cell Receptor

1. Summary

With almost 39 million infected people worldwide and a lack of curative therapy options, HIV infection still plays an important role in our health system, as well as in research. The human immune response generally fails to control HIV-1 infection and to target the HIV-1 reservoir and despite decades of research, both an effective HIV-1 vaccine and a curative therapy remain elusive.

The most successful measure to date in the treatment of HIV-1 infection is antiretroviral therapy, which suppresses the virus plasma level. This lifelong therapy could significantly reduce the imortality rate and led to an almost normal life expectancy. However, a cure has not been achieved. so research into new and innovative therapeutic approaches, in addition to preventive strategies, is still necessary.

Chimeric antigen receptor (CAR) T cells are a promising approach. These genetically modified T cells are engineered to bypass regular HLA- dependent mechanisms of T cell activation. Antigen-binding of CAR T cells is typically achieved by employing antibody-derived single chain variable fragments (scFvs). These scFvs are engineered proteins expressed on the surface and they retain the antigen-recognition specificity of the original antibody, allowing CAR T cells to target specific cell surface antigens.

Recently identified highly potent broadly neutralizing antibodies (bNAbs) targeting conserved envelope epitopes are defined by their remarkable neutralization activity against many globally circulating HIV-1 strains. In early phase clinical trials, bNAbs were generally well tolerated and demonstrated significant antiviral activity in viremic HIV-1-infected individuals, highlighting the great potential of immunotherapy of HIV-1 infection.

The aim of this work is a systematic investigation of bNAb derived scFvs to test their suitability as a possible binding site of CAR T cells and to gain information about scFv affinity and specificity leading to enhanced CAR T cell persistence and efficacy.

Ten potent neutralizing antibodies which bind to different epitopes on the HIV surface protein including the CD4 binding site, the V1/V2 loop, the V3-stem, and the Membrane Proximal External Region (MPER), as well as CD4 and a control antibody were generated in order to characterize the properties of the scFv antibodies and to compare them with the respective IgG4 and IgG1 antibodies. The antibody constructs were tested in different assays, as well as in a non-humanized mouse model.

The results demonstrated that binding characteristics of bNAb-derived scFvs are only slightly weakened compared to full-length antibodies when measured by ELISA and flow cytometry. Moreover, autoreactive properties determined by a HEp-2 cell assay showed similar results for

the antibody constructs. However, the neutralization activity of full-length antibodies against different HIV-1 strains were higher. Furthermore, it could be shown that the generated scFv and IgG4 antibodies achieved longer half-lives after intravenous injection in non-humanized mice compared to the IgG1 antibodies. At last, a humanized mouse model was established to study new treatment approaches and immune responses.

Overall, it could be shown that scFvs offer promising features as a binding domain of bNAb-derived CAR T cells and the results form the basis for the that scFvs are a crucial component of CAR T cells, allowing for the specific recognition and binding of target antigens.

2. Zusammenfassung

Mit weltweit fast 39 Millionen Infizierten ist die HIV-1-Infektion nicht nur ein bedeutendes Thema in den globalen Gesundheitssystemen, sondern spielt auch in der Infektionsforschung eine bedeutende Rolle. Eigenständig ist das menschliche Immunsystem nicht in der Lage die HIV-1-Infektion zu kontrollieren und das latente Reservoir zu eliminieren.
Die bislang erfolgreichste Maßnahme in der Behandlung der HIV-1-Infektion ist die antiretrovirale Therapie. Erkrankte müssen hierfür täglich eine Kombination aus verschiedenen Medikamenten einnehmen, die das Virus-Plasmalevel unterdrücken. Diese lebenslang einzunehmende Therapie kann die Sterberate erheblich senken und führt zu einer nahezu normalen Lebenserwartung. Eine Heilung der Krankheit konnte allerdings bislang nicht erreicht werden. Die Erforschung neuer und innovativer Therapieansätze ist neben Präventionsstrategien daher weiterhin dringend erforderlich.
Ein vielversprechender Ansatz sind Chimäre Antigenrezeptor (CAR)-T-Zellen als neue Therapiemöglichkeit. Diese genetisch veränderten T-Zellen können reguläre HLA-abhängige Mechanismen der T-Zell-Aktivierung umgehen. Die Antigenbindung wird durch sogenannte Einzelstrang-Antikörper (single chain variable fragments (scFv)) ermöglicht, welche jeweils aus der variablen schweren und leichten Kette eines Antikörpers bestehen, und auf der Zelloberfläche exprimiert werden. Hierdurch wird die Antigenspezifität des ursprünglichen Antikörpers beibehalten und die Bindung spezifischer Zelloberflächenantigene ermöglicht.
Das Ziel dieser Arbeit ist die systematische Untersuchung der scFvs, um ihre Eignung als mögliche Bindungsstelle von CAR-T-Zellen zu testen und Informationen über die Affinität und Spezifität von scFvs zu gewinnen.

Auf Basis von bereits bekannten, breit neutralisierenden Antikörpern, wurden insgesamt zehn Antikörper, die an unterschiedlichen Epitopen des HIV - Oberflächenproteins binden als scFv, IgG4 und IgG1 Variante generiert, um so die Eigenschaften zu charakterisieren und mit den jeweiligen IgG4 und IgG1 Antikörpern zu vergleichen. Die Antikörperkonstrukte wurden in verschiedenen Assays, sowie in einem nicht-humanisierten Mausmodell getestet.

Die Ergebnisse haben gezeigt, dass alle Einzelstrang-Antikörper lösliches und zell-oberflächen gebundenes Protein binden. In einem Neutralisationsassay wurden höhere Konzentrationen der Einzelstrang-Antikörper benötigt, um eine vergleichbare Neutralisationsaktivität gegen vier verschiedene HIV-1 Pseudoviren zu erreichen. In einem klinisch geprüften Autoreaktivitätstest konnte kein wesentlicher Unterschied zwischen den verschiedenen Antikörper-Gruppen gezeigt werden. Eine Mutation in der konstanten Domäne der scFv und IgG4 Antikörper konnte die Halbwertszeit nach intravenöser Injektion in nicht-humanisierten Mäusen verlängern im Vergleich zu den jeweiligen IgG1 Antikörpern. Weiterhin

wurde ein humanisiertes Mausmodell etabliert, um neue Behandlungsansätze *in vivo* zu testen.

Insgesamt konnte gezeigt werden, dass sich die Einzelstrang-Antikörper basierend auf breit neutralisierenden Antikörpern als Bindungsdomäne von CAR-T-Zellen eignen und vielversprechende Eigenschaften bieten, sodass die spezifische Erkennung und Bindung von Zielantigenen ermöglicht wird.

3. Introduction

3.1 Human Immunodeficiency Virus (HIV)

In 1983 researchers discovered a new human T-lymphotropic retrovirus, named HTLV-III, causing a severe acquired immunodeficiency syndrome (AIDS) in a group of young homosexual men in the United States. Shortly afterwards, further risk groups and risk behavior were identified, including blood transfusions and intravenous drug abuse[1-4]. The virus was initially subordinated to the HTLV family, a group of retroviruses targeting mature T helper cells leading to leukemia and immunodeficiencies in infected patients[5]. Five years later, the International Committee on Taxonomy of Viruses (ICTV) agreed to rename the virus to human immunodeficiency virus (HIV). It was found that HIV originates from simian immunodeficiency virus (SIV), discovered in African nonhuman primates. Two distinct viruses; HIV-1 and HIV-2, were transmitted to humans from this species, probably through cutaneous and mucosal exposure with blood. Therefore, this viral infection was assigned to the zoonoses[6]. It was found that three subgroups of HIV-1 showed a matching genomic structure as SIVcpz, transmitted from chimpanzees in Cameroon, representing a natural host of this virus[7]. On the other hand, it could be shown, that HIV-2, found in sooty mangabey monkeys, can be attributed phylogenetically to SIVsm, which was initially identified in sooty mangabey monkeys[6,8,9]. However, to this date, it is difficult to understand when and where the first cross-species transmission took place.

While HIV-2 infections mainly occurred in west Africa, HIV-1 led to a global pandemic with at least 80 million infections until today[10,11]. HIV-1 is divided in different subgroups based on their sequence. These groups could later be assigned to the initial transmission event. Group M, N and O were found in chimpanzees and group P could be detected in gorillas[12,13]. Group M is the most relevant of the above mentioned. Nine subtypes have been found to belong to this group. Subtypes A, C, D, F, G, H, J and K are mostly found in Africa and India. Subtype B predominates in Europe, America and Australia[14]. Subtype C is responsible for 48% of the HIV-1 infections worldwide.

3.1.1. Epidemiology

38.4 million people worldwide are infected with HIV these days. The greatest prevalence can be found in sub-Saharan Africa with 20.6 million as well as in southeast Asia with 6 million infected persons. Though the rate of new infections declined by 32% since 2010, still 1.5 million new HIV infections were detected in 2021[15]. This necessitates more and profound prevention strategies and education, especially for at-risk groups, as well as deeper understanding of virus transmission. Due to the development of antiretroviral therapies and their increased accessibility, especially in middle- and low-income countries like Africa, but also due to

education and other preventive measures, the HIV-related mortality decreased[10,16]. It could be observed that particularly the infection rate in children declined, because of efforts to reduce the mother-to-child transmission[10]. Nowadays,75 % of all infected persons worldwide receive an antiretroviral therapy (ART)[17]. This antiviral treatment, which consists out of a combination of different drugs based on their molecular mechanism, is able to suppress the viral load to undetectable level, however must be taken lifelong on a daily basis[18].

Risk groups for HIV infections remains men who have sex with men (MSM), people who abuse drugs, female sex workers and their clients as well as people in prison, because of unsafe sex and intravenous injections[19-22]. Almost 50 % of the causes of death in HIV-infected people are caused by AIDS-related diseases[23]. Especially, people living in low-income countries might die because of co-infection with mycobacterium tuberculosis[24]. The broad availability of antiretroviral medication could successfully decrease the AIDS-related mortality of people living with HIV in high-income countries, where main causes of deaths are associated with cardiovascular diseases, liver diseases and cancer[10,23]. Nevertheless, the global burden of HIV must not be neglected, and it is necessary to work towards a cure.

In Germany, 87.000 people are infected with HIV, whereby less than 200 children between 0 and 14 years are affected. Thus, there is a prevalence rate of 0.1 % in Germany. The latest data from 2018 revealed an incidence of 0.03 % with 2600 new infections in all ages. Since 2010 the rate of new infections decreased by 9 %. In addition, Germany recorded fewer that 500 deaths due to AIDS. The coverage of all ages receiving ART is estimated around 75 %[15].

3.1.2. Transmission

HIV is either transmitted through mucosal exposure, exposure to blood or vertical from mother to infant. In adults, 80% are transmitted through mucosal membranes, including rectal, penile, and oral mucosae but also the gastrointestinal tract, where the virus can infect $CD4^+$ T cells, dendritic cells and macrophages after crossing the epithelial barrier[25-29]. A few days after exposure, the infected cells are migrating to lymphoreticular tissues, leading to a systemic dissemination with $CD4^+$ T cell depletion[30]. $CD4^+$ T cells are normally responsible for the adaptive immune response, e.g., activation of macrophages, and coordination of B and T cells[31,32]. In HIV infection, the CD4 receptor interacts with the envelope protein of the virus and allows viral entry. Why T cell depletion particularly takes place in gut associated lymphoid tissues and other lymphoid tissues like lymph nodes is not yet fully understood. An explanation could be the proportion of present $CD4^+$ T cells and the enhanced expression of HIV co-receptors like CCR5 and CXCR4 on the cell surface compared to lymphocytes in peripheral blood[33-35]. The chemokine receptors, CCR5 and CXCR4, are required for the infection and they promote in addition to the CD4 receptor the fusion of the virus and target cell membranes[32,36]. In the early stages of infection, a latent reservoir is established in these lymphoid tissues[37].

They entail resting $CD4^+$ T cells harboring replication-competent proviruses. Since these latently infected cells do not produce virus, they will not be recognized by the immune system. This also leads to the inability of ART to attack these latent cells and is also critical for cessation of therapy, since it could lead to a rebound of viremia[38-40]. Immediate intake of ART after infection might be crucial for the extent of the latent reservoir[41]. Nevertheless, latency of virus is an obstacle for ART, because it is unlikely to eradicate it and therefore to cure it[42]. New therapies such as the "shock and kill" strategy is required. This treatment involves latency reversing agents (LRA) to induce - expression, of the provirus which is followed using immune mechanisms to efficiently eradicate the t infected cells[43,44].

Cytotoxic lymphocytes (CTL) play an essential part in an effective immune response and are capable to control acute and chronic HIV infection through cytokine production and lysis of infected cells[45,46]. These $CD8^+$ T cells are essential for viral remission at the beginning of the infection, as they limit the initial replication and are responsible for establishing the viral setpoint, a stable level of viral load after the first peak of acute infection[25,47,48]. But it was shown that antigen-specific stimulation of CTLs might induce eradication of HIV infected cells which might be necessary for eliminating the latent reservoir[31,49,50]. This underlines the importance of cellular immunity[51]. During HIV infection, the virus develops escape mechanisms to evade the CTL response, thereby viral proteins induce a human leukocyte antigen (HLA)-downregulation, which is required for the antigen presentation to CTLs[50,52-54]. HLAs can be found on every cell surface and are essential for the interaction of different immune cells[55]. Furthermore, during infection a T cell exhaustion is induced through PD-1 upregulation with necroptosis of $CD8^+$ T cells, which eventually leads to disease progression[56-59].

3.1.3. HIV Envelope Protein

The HIV-1 envelope protein consists of a trimer of gp160, a glycoprotein which is cleaved in two subunits, the surface glycoprotein gp120 and the transmembrane protein gp41. Gp41 is responsible for the fusion of the virus with the host cell membranes and gp120 interacts with the hosts cell surface receptors CD4 and coreceptors CCR5 and CXCR4[60,61]. Antibodies against gp41 are built in the first two to four weeks after HIV-1 infection and afterwards the human immune system produces anti-gp120-antibodies, which can be detected approximately three weeks after infection the earliest[62]. The exact structure of the envelope protein is particularly interesting for the development of antibody-based therapies to prevent viral infection. There are essentially four major surface protein binding sites that have been identified, the V1/V2 loop, the V3 glycan, CD4 binding site and the membrane proximal external region (MPER). These epitopes are recognized by most antibodies. However, only 14 envelope spikes are presented on the viral surface, furthermore the epitopes are surrounded

by *N*-glycans, which build a glycan shield to protect the underlying surface protein and to overcome the host immune system[63,64].

3.1.4. Antiretroviral Therapy

The development and administration of ART allowed to treat HIV-1 infection as aoften-well-chronic disease. A combination of different drugs has proven to be effective for HIV treatment including nucleoside reverse transcriptase inhibitors, non-nucleoside reverse transcriptase inhibitors, protease inhibitors and integrase inhibitors[65]. In addition, ART can prolong disease progression and suppress viremia, but patients must commit to lifelong and frequent administration of antiretroviral drugs and adverse effects without achieving cure because of viral latency[66-68]. Common side effects include gastrointestinal symptoms like diarrhea and nausea, osteoporosis, renal insufficiency, depression, and psychosis as well as dyslipidemia[65]. Nevertheless, new treatment approaches are of pivotal necessity, since persistence of replication-competent provirus in resting $CD4^+$ T cells remains a hurdle for ART. Additionally, ART can become ineffective in case of viral resistance. Cellular and antibody-based therapies are needed and might be the only option to eliminate the HIV-1 reservoir and eventually overcome the barrier of cure[69-71].

3.2 Broadly Neutralizing Antibodies (bNAbs)

The search for a vaccine against HIV-1 was started straight after the discovery of the virus[72]. In 1994, a specific antibody was found to have a neutralization activity of 75% and targeting the glycoprotein gp120 on the envelope of HIV-1[73]. Major efforts have been made to find a cure and to prevent HIV infection, but the low expression of the viral envelope protein (Env), the unstable conformational state and the amount of different HIV strains aggravated the progress towards a cure[61,74]. A few years later, after examining numerous isolated antibodies from infected persons, there were only very few who formed particularly effective antibodies[75]. New technologies like single B cell sorting allowed to isolate these very potent and broad neutralizing antibodies[76-79]. These antibodies can effectively neutralize a broad range of viral strains with a high potency, which means they can either inhibit viral entry in cells or through an antibody dependent cell mediated cytotoxicity[75]. Because of their properties, such as their high specificity, bNAbs administer immune pressure on the virus which eventually results into escape mutations[80]. These mutations lead to changes in the env gene, which develop resistant viruses preventing bNAb binding[81].

3.2.1. Characteristics of bNAbs

Antibodies play an important role in viral infections. They interact with the envelope protein of the virus and thus avoid further infection of the hosts $CD4^+$ cells. On the other hand, the Fcγ receptor interacts with antibody labeled virus and infected cells and activates host immune cells (macrophages, NK cells), which eventually leads to lysis of the infected cells. Furthermore, bNAbs are characterized by having somatic hypermutations, structural features like a long complementarity determining region (CDR3) as well as polyreactivity[76,82]. At this time, it cannot be precisely predicted who and why people form these antibodies. Some contributing factors might be the plasma viremia levels and time since infection[83]. Many bNAbs have been isolated until today, which vary in their potency and their binding site on the virion surface. The main binding sites are the CD4-binding site, the MPER, the *N*-linked glycan-containing epitopes (Figure 1) and a few more are still being researched[60]. It could be shown that the binding pattern is relevant for antibody treatment, since the combination of two different bNAbs in HIV-1 infected individuals reduced the probability of escape mutations and increased the neutralization breadth similar as it applies to ART[84,85]. This approach can also be applied to CAR T cells. Several groups developed bispecific or duoCARs, which target multiple epitopes to control viremia and prolong the *in vivo* persistence[86,87].

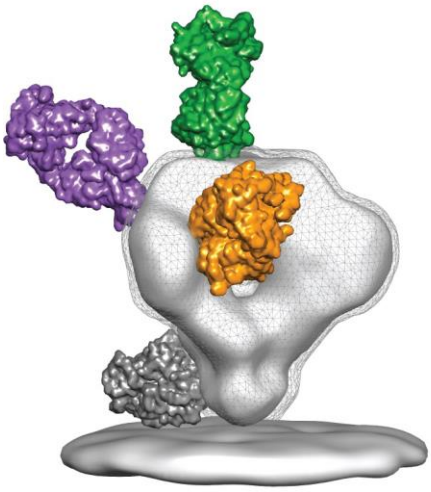

V1/V2 Loop
• PGT145
V3 Glycan
• 10-1074 • 1-79
CD4 Binding Site
• 3BNC117 • NIH4546
MPER
• 10E8 • 4E10
gp120/41 Interface
• PGDM1400 • 8ANC195 • 3BC176

Figure 1: Antibody binding sites on the HIV envelope protein.

As described above the HIV-1 envelope protein consists of a trimer of gp160, which is cleaved in two subunits, the surface glycoprotein gp120 and the transmembrane protein gp41. Shown is an EM-based illustration of the envelope protein showing color-coded binding sites including the V1/V2 loop in green, the V3 glycan in purple, CD4 binding site in orange, the MPER in grey. Exemplary antibodies that bind to the respective binding sites are listed on the right-hand side (modified from Klein, F et al., Science, 2013).

3.2.2. Clinical Application of bNAbs

First *in vivo* experiments in humanized mice could show that the administration of neutralizing antibodies simultaneously to viral challenge prevented HIV-1 infection, but they could not control an established infection followed by viral escape[88]. A few years later, more potent broadly neutralizing antibodies have been isolated by single cell sorting and the application in HIV-1 infected humanized mice and non-human primates could decrease viral load to undetectable limits[85,89]. Administration of 3BNC117, a CD4-binding site antibody, and 10-1074, targeting the V3 glycan, a *N*-linked glycan epitope, alone or in combination in HIV-1 infected individuals, revealed safety and effectiveness, indicating that bNAbs may be relevant for prevention and therapy of HIV-1 infection[90-92]. Whether bNAbs can attack the latent reservoir is not entirely ensured. Some bNAbs like 3BNC117 might be able to kill latently infected cells[93]. Another approach would be to combine bNAbs and LRA to activate those infected cells. First

in vivo results showed sustained suppression of viral rebound after cessation of ART[94-96]. But it could also be shown, that 3BNC117 and romidepsin, a latency reversing agent, did not have a relevant influence on the latent reservoir tested in people on ART[97]. Additionally, it should be considered that administering of bNAbs could cause development of escape mutations of the virus[91]. Treatment with a single bNAb can effectively reduce viremia, but only for a certain amount of time. Administration of a combination of different bNAbs was more efficient and development of resistance was more difficult[84]. Therefore, viral strains should be monitored on regular basis, since it may have an impact on the outcome of clinical trials[93]. Overall, the results suggest that bNAbs alone or in combination might not be sufficient to eliminate the latent reservoir.

3.3 CAR T Cells

For eradication of acute viral infections, a functioning cytotoxic T cell response is required, as T cells are capable to lyse HIV infected cells and induce cytokine production[31,98]. Chimeric antigen receptor (CAR) T cells are genetically modified T cells, that target cell-surface epitopes typically through an antibody-derived scFv. They represent an appropriate alternative as an adoptive T cell therapy, allowing MHC-independent recognition of antigens[99]. It offers a combination of target specificity and T cell effector functions and therefore a new approach to treat different diseases. A paragon for the design of CARs is the use of a $CD19^+$ CAR in B cell malignancies. CD19 can be found on the surface on almost all B cell lineages and is therefore a suitable target to treat hematological malignancies[100,101]. In multiple clinical studies, it could be shown that the infusion of patient derived genetically modified CAR T cells is able to achieve remission in these patients with refractory B cell lymphoma and leukemia[100,102,103]. In 2017, the first adoptive cell therapy (ACT) using $CD19^+$ CAR was eventually approved by the United States Food and Drug Administration (FDA) for treatment of patients with relapsed or refractory B cell precursor Acute Lymphoblastic Leukemia (ALL)[104]. In the meanwhile, Liu et al. generated VRC01 CAR T cells and treated fifteen HIV-1 infected persons in a phase I clinical trial. CAR T cell infusion led to reduction of viral RNA which could be sustained between three to ten weeks[105].

3.3.1. T Cell Receptor/CD3 Complex

First developments of CARs were based on the design of TCR. The T cell receptor/CD3 complex consists of extracellular α and β chains, linked to CD3 dimers $CD3\varepsilon\gamma$, $CD3\varepsilon\delta$ and $CD3\zeta\zeta$ (Figure 2). The TCR mediates the recognition of antigens bound to MHC molecules, while the CD3 molecules transmit activation signals to the T cell[106,107,108,109].

3.3.2. Design of CARs

The CAR is a complex construct, consisting of different domains which are separated in extracellular and intracellular parts (Figure 2). The extracellular binding domain is responsible for the interaction with the antigen and is investigated in this doctoral thesis. To understand the full functionality of the CAR, information about the history and structure of the receptor are provided in detail below.

3.3.3. Ectodomain

Using an antibody-derived targeting domain, the CAR T cell can be directed towards any protein on the cell surface, and it can bind to carbohydrate and glycolipid structures as well[110,111]. To bind specific antigens like tumor cell surface molecules, a single chain variable fragment (scFv) consisting of the variable light and variable heavy chain of a monoclonal antibody are used to achieve a high affinity to the target[112,113]. Antigen processing is not required, and it has been shown that CARs obtain much higher affinity to their antigens compared to TCRs. In addition to that, TCRs bind much weaker to auto antigens compared to foreign ones[114,115]. Using scFvs allows MHC-independent and high affinity binding as well as efficient stimulation of the T cell[113]. The signaling domain is followed by a spacer region, which is crucial for a potent T cell function, as well as for the length and flexibility of the CAR T cell and is usually derived from CD8 or the constant domain of IgG4 or IgG1[113,116,117]. The constant region of immunoglobulins interacts with receptors (FcRs) on immune cells like macrophages to enable immune functions[118,119]. This hinge region is responsible for the distance from the binding domain to the cell surface. There are different theories how long the hinge region should be to elicit efficient functions in an *in vitro* assay or in an *in vivo* model, since a short spacer region induced a superior T cell function, including higher cytokine levels and advanced T cell proliferation, compared to constructs with long spacer regions which might also depend on the targeted antigen[120].

3.3.4. Endodomain

The transmembrane domain links the extracellular and the intracellular part of the receptor. Derived from CD28, CD8α, CD4 or CD3ζ, it not only builds a structural part but also has impact on the effector function of the T cell comparable to the hinge region[116]. The investigation of different domains is important, since it could be shown, that a CD3ζ transmembrane domain loses its stability over time compared to a 2nd generation CAR[121].First-generation CARs with CD3ζ chain derived from TCRs were able to elicit an immune response. Though, repeated antigen stimulation decreased levels of cytokines and the proliferation of T cells[122]. Second-generation CARs were then used to reach an improved expansion, since it was shown, that

the amount of co-stimulatory domains of the intracellular part of the CAR T cell leads to differences in the effectiveness, expansion and persistence of the cells[121]. CD28, 4-1BB, DAP10 and OX40 are only a few domains used for co-stimulation and they can vary in their configurations and potency[123-125]. Some results might indicate that the generation of CARs with two co-stimulatory domains, called third-generation CAR, shows superiority compared to only one co-stimulation domain[126,127].

In summary, newer generations of CAR T cells are able to achieve greater activation through multiple stimulatory domains and thus enhance the expression of cytokines.

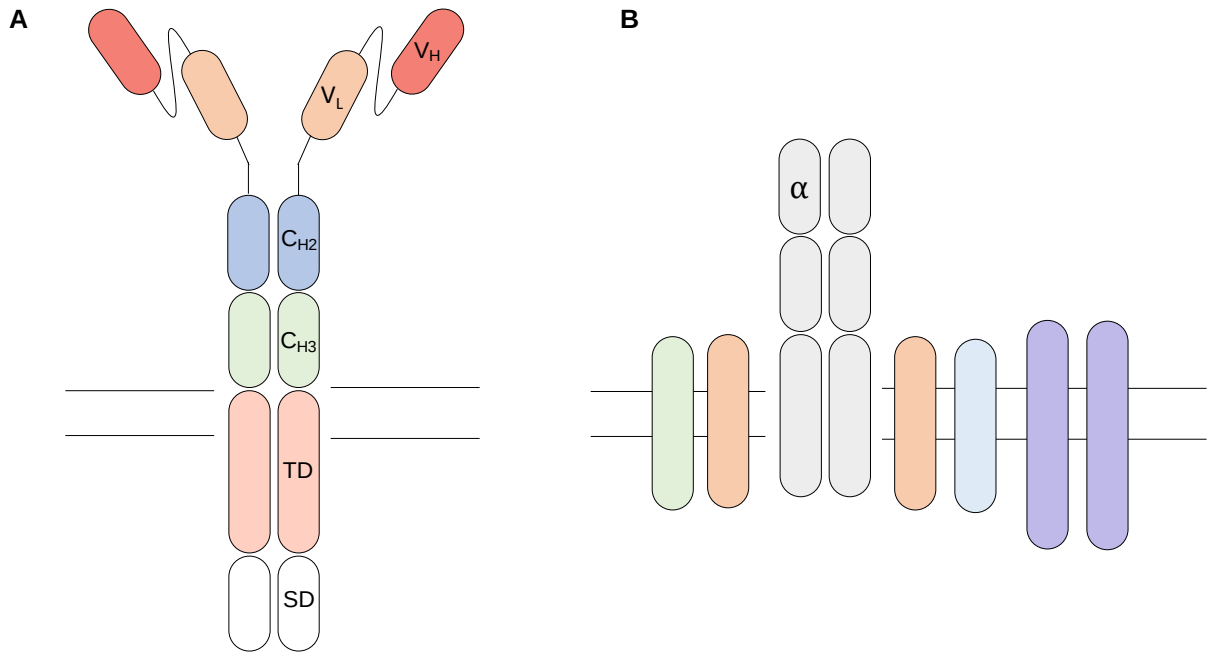

Figure 2: Schematic representation of CAR and T cell receptor.

(A): The extracellular part of the CAR is composed of scFv, as the targeting domain, consisting of the variable light (VL) and variable heavy chain (VH) of a monoclonal antibody. Followed by a spacer region which is often derived from CD8 or the constant domain of IgG4 or IgG1 (CH2, CH3). The transmembrane domain (TD) is then followed by the intracellular stimulation domain (SD). **(B)**: The T cell receptor/CD3 complex consists of extracellular α and β chains, linked to CD3 dimers CD3$\varepsilon\gamma$, CD3$\varepsilon\delta$ and CD3$\zeta\zeta$.

3.3.5. Anti-HIV-1-CAR

First approaches to treat HIV-1 infection and to induce a greater T cell response *in vitro*, have been achieved through transferal of HIV-1 specific T cell receptor (TCR) chains into affected human T cells[128]. Furthermore, early attempts of using CAR T cells against HIV-1, were already performed in clinical trials about 25 years ago. Genetically modified $CD4^+$ and $CD8^+$ T cells were administered after *ex vivo* expansion in single and multiple infusions in a HIV-1 infected individual. Biopsies of lymph nodes revealed the trafficking of the infused cells to lymphoid tissues. This anti-HIV-1 CAR with a CD4 molecule was well tolerated in humans but showed no significant antiviral effect[111,129]. This anti-HIV-1 CAR used the CD4 molecule as the extracellular and transmembrane domain, which binds to gp120 expressed on infected cells, furthermore CD3ζ of TCR build the signaling domain[130]. Nevertheless, this new approach demonstrated safety and longevity of infused CAR T cells. However, there are also some case reports of serious side effects after administration of CAR T cells like cytokine release syndrome (CRS)[131].

The discovery of potent broad neutralizing antibodies against HIV-1 offered new opportunities to develop more potent CAR T cells. First results could show that anti-HIV-1 CAR T cells elicit an efficient antiviral activity [70,87,111,132].

3.3.6. Need for Control of CAR T Cell Therapy

CAR T cells offer an interesting and exciting approach for treatment of various diseases including cancer and viral infections[133-135]. Furthermore, it is important to assure that the binding domain retains its antigen specificity and no off-target toxicity is induced[136]. Hence, it is important to undergo an extensive toxicity screening of the respective CAR construct before approval[131]. Neurotoxicity and CRS are common toxicities observed in patients after receiving $CD19^+$ CAR T cells. A high tumor burden as well as the CAR T cell dose have turned out to be an increased risk factor for development of these side effects[137,138]. The increase of cytokine serum levels including interleukin-6 (IL-6), IL-1 and interferon γ (IFN-γ) defines the CRS, which eventually leads to an increase of the microvascular permeability and an activation of the endothelium resulting in fever, hypotension, and organ failure. To control circulating CAR T cells, researchers developed a safety tag, that is expressed additionally on the cell surface. This epidermal growth factor receptor (EGFR) can be detected for cell persistence by immunohistochemistry and flow cytometry analysis. Furthermore, in severe cases of toxicity CAR T cells can be depleted by application of an anti-EGFR-antibody like cetuximab[112,139]. However, the efficacy of the therapy might be reduced after depletion[137]. Furthermore, immunosuppressive therapies like corticosteroids or monoclonal antibodies like Tocilizumab, targeting IL-6, have been shown to reverse the symptoms[140].

3.4 Use of small animal models in HIV research

Small animal models, like mice and non-human primates have been instrumental in advancing HIV-1 research. Particularly mice have been used to study the mechanisms of viral replication, immune responses und the pathogenesis. Furthermore, small animal models allow to test new drugs and study vaccine design *in vivo*, as well as antibody-based therapies. Especially the development of humanized mouse models can provide insights into the safety and efficacy of new treatment approaches[141,142]. Humanized mice are developed to mimic the human immune system through transplantation of human tissues or cells and have become an integral part of current research[85].

3.5 Aims, Objectives and Hypothesis of the Thesis

To this date, many bNAbs against HIV have been identified and are widely studied. Since scFvs are known to be good candidates as a target domain for CAR T cells, the aim of this doctoral thesis was to generate scFvs based on known bNAbs. Since their properties and behavior differ from IgGs, their potential suitability must be examined. The behavior was evaluated *in vitro* and *in vivo* to find out which characteristics are substantial for the most potent and suitable antibody for the generation of anti-HIV-1 CAR T cells. Furthermore, to facilitate the analysis of HIV-1 treatment is the availability of *in vivo* models[142,143]. Thus, an additional aspect of this thesis is focused on the establishment of a humanized mice model using placental tissue and cord blood derived stem cells. In summary, the following objects were addressed in this thesis:

1. The generation of twelve different scFv constructs and their respective full-length IgG1 and IgG4 antibodies.

2. The characterization of the generated antibodies in different *in vitro* assays and the determination of the *in vivo* half-life in non-humanized mice.
   - HIV-1-Env ELISA
   - Cell Surface Binding
   - Half-life determination in non-humanized mice
   - HEp-2 Cell Immunofluorescence Assay
   - Neutralization Assay

3. Establishment of a humanized mouse model and systemic analysis of the humanization efficiency from placenta tissue and umbilical cord blood.

4. The evaluation of the results and eventually the selection of the most promising candidate for generation of anti-HIV-1 CAR T cells.

4. Materials and Methods

4.1 Materials

The materials and resources used in the experiments are listed in the following table.

Table 1: Materials and resources table

Reagent	Source	Cat. No.
Antibodies		
Peroxidase AffiniPure Goat Anti-Human IgG, Fcγ Fragment Specific	Jackson Immuno Research	109-035-098
Goat Anti-Human IgG-AF647 1,0 mg	Biozol	SBA-2040-31
AffiniPure Goat Anti-Human IgG	Jackson Immuno Research	109-005-098
Anti-Human CD45, Pacific Orange	Thermo Fisher Scientific	MHCD4530
Anti-Human CD16, Alexa Fluor 700	BD	557920
Anti-Human CD3, Pacific Blue	BD	558117
Anti-Human CD4, PE	BD	340419
Anti-Human CD8, FITC	BD	345772
Anti-Human CD19, APC	BD	555415
Anti-Mouse CD45, PE/Cyanine7	BioLegend	103114
Bacterial and virus strains		
One Shot; Stbl3; Chemically Competent E. coli	Invitrogen	C737303
E. coli DH5α		
HIV-1 Env Pseudoviruses	NIH Reagent Program, Schommers, Gruell [144]	12670
Murine Leukemia Virus (MuLV)	Schommers, Gruell [144]	N/A
Biological samples		

Human $CD34^+$ Stem cells isolated from placental tissue	Department of Gynecology and Obstetrics, University Hospital of Cologne	N/A
Chemicals and proteins		
FreeStyle TM 293	Gibco	12338-026
Dulbecco's Modified Eagle Medium (DMEM)	Gibco	11960-044
RPMI 1640 Medium	Thermo Fisher Scientific	11530586s
LB Medium (Tryptone, Sodium Chloride, Yeast Extract, H2O)	Carl Roth	8952, 3957, 2363
Trypsin-EDTA 0,25%	Thermo Fisher Scientific	25200056
Fetal bovine serum (FBS)	Sigma Aldrich	F9665
Sodium Pyruvate	Gibco	11360070
L-glutamine	Gibco	25030081
Penicillin/Streptomycin	Gibco	15140122
Antibiotic/Antimycotic	Gibco	15240062
ABTS solution	Thermo Fisher Scientific	002024
DAPI	Thermo Fisher Scientific	D1306
Cell Dissociation Buffer, enzyme-free	Thermo Fisher Scientific	13151014
Bovine serum albumin (BSA)	Sigma Aldrich	A2153
Polyethylenimine (PEI)	Sigma Aldrich	408727
Roti Blue	Carl Roth	A152
SDS	Carl Roth	0183
Ampicillin	Carl Roth	K029.2
Gentamicin	Sigma Aldrich	G1397
Protein G Sepharose 4 Fast Flow	Sigma Aldrich	17-0618-05
Ni-NTA Agarose	Macherey-Nagel	745400.25
HEPES	Millipore	L1613
PBS 1x	Gibco	10010-015
Tween 20	Carl Roth	9127.1
Phusion High-Fidelity DNA Polymerase	New England Biolabs	M0530S
dNTP Mix (25 mM each)	Thermo Fisher Scientific	R1121

Taq DNA Polymerase	Qiagen	201203
Platinum Taq High Fidelity	Thermo Fisher Scientific	11304011
S.O.C. Medium	Thermo Fisher Scientific	15544034
T4 DNA Ligase	New England Biolabs	M0202 S
SYBR Safe DNA gel stain	Thermo Fisher Scientific	S33102
AgeI-HF	New England Biolabs	R3552L
BamHI-HF	New England Biolabs	R3136S
EcoRI-HF	New England Biolabs	R3101S
BsiWI-HF	New England Biolabs	R3553S
DEAE-Dextran	Sigma Aldrich	93556
CountBright Counting Beads	Thermo Fisher Scientific	C36995
Experimental models		
Cells lines		
HEK293T cells	ATCC	CRL-11268
HEK293-6E cells	National Research Council of Canada	NRC file 11565
TZM-bl cells	NIH AIDS Reagent Program[145]	8129
Animal models		
NOD-Rag1^{null}IL2rg^{null} (NRG) mice	The Jackson Laboratory	007799
Commercial kit		
NOVA Lite HEp-2	Inova	066708100
HiPure Plasmid Filter Purification Kits (Maxi Prep)	Invitrogen	K2100-16
QiaPrep Miniprep	Qiagen	27106X4
SDS PAGE Prep Kit	Thermo Fisher Scientific	89888
PCR Clean Up Kit	Macherey Nagel	740609.50
NuPAGE Bis-Tris Gel	Invitrogen	NP0335PK2
Other		
Ultrafree-MC columns	Merck Millipore	UFC30GV0S
Amicon Ultra-15 tubes	Merck Millipore	UFC901024
Safe-Lock Tubes 1.5 mL	Eppendorf	0030120086
High Binding ELISA Plates	Corning	3690
Micro Sample Tubes Serum Gel 1.1 mL	Sarstedt	41.1378.005

4.2 Methods

4.2.1. Mouse Models

NOD-Rag1^{null}IL2rg^{null} (NRG) mice were obtained from The Jackson Laboratory and bred at the Decentralized Animal Husbandry Network (Dezentrales Tierhaltungsnetzwerk) of the University of Cologne under specific pathogen free (SPF) conditions. The temperature range was between 20 to 24 °C and an automated light cycle of 12-12 hours (light-dark) was maintained. Mice were fed ad libitum with gamma-irradiated animal feed (ssniff 1124 and 1543) and were also supplied with acidified water ad libitum. All protocols of the study were designed and performed in strict accordance with the European Union guidelines, established by the European Community Council Directives 86/609/EEC (European Council, 1986), concerning the protection of experimental animals, with approval by the State Agency for Nature, Environmental Protection, and Consumer Protection North Rhine-Westphalia (LANUV) (AZ 84-02.04.2015.A353). Experiments were performed according to the ARRIVE guidelines[146].

4.2.2. Cell Lines

HEK293T cells (American Type Culture Collection) were cultivated in Dulbecco`s Modified Eagle Medium (DMEM, high glucose, no glutamine, Gibco) containing 10% fetal bovine serum (FBS) (Sigma Aldrich), 2 mM L-glutamine (Gibco), 1 mM sodium pyruvate (Gibco) and 1% antibiotic-antimycotic (Gibco) at 37 °C and 5% CO_2. 293-6E cells (National Research Council of Canada) were cultivated at 37 °C and 6% CO_2 in FreeStyle Expression Medium (Gibco) under constant shaking at 90-120 revolutions per minute (rpm).
TZM-bl cell line expressing CD4, CXCR4 and CCR5[145] were kept at 37 °C and 5% CO_2 in DMEM containing 10% FBS, 2mM L-glutamine, 1 mM sodium pyruvate, 25 mM Hydroxyethyl-piperazineethanesulfonic acid (HEPES, Millipore) and 50 µg/mL gentamicin (Sigma Aldrich).

4.2.3. Cloning of scFv and Full-length Antibody Plasmids

Ten well-known neutralizing antibodies against HIV-1 (10-1074, 3BNC117, PGT145, PGDM1400, NIH45-46, 4E10, 10E8, 8ANC195, 3BC176 and 1-79), CD4 (composed of domains 1 and 2) and BW431/26, a humanized anti-CEA scFv with CH2/CH3 constant human IgG domains[147], were chosen for generation and analysis of single chain variable fragments (scFv) as a potential binding domain for an anti-HIV-1-CAR. Antibody sequences of full-length IgG1 antibodies were acquired from GenBank. To generate the scFv-Fc expression vector of the respective full-length antibody, the leader and IgG1 constant region of the antibody

expression vector were removed by restriction digest and new restriction sites, as well as a modified human IgG4 constant region, were introduced[148]. The modified human IgG4 region was introduced to prolong the half-life of scFv constructs and IgG4 full-length antibodies. It contains missense mutations to substitute amino acids for a stabilized hinge region and reduced Fc-binding (L>E; N>Q; S>P)[119,149].

The scFv constructs are composed of the variable heavy chain, followed by a linker sequence and the variable light chain including the modified IgG4 region. These are introduced into the new generated scFv-Fc expression vector through restriction digest via the restriction sites AgeI and ApaI (New England Biolabs) according to the manufacturer`s protocol. For further generation of modified IgG4 antibodies, different restriction sites to introduce the variable light (kappa or lambda) and variable heavy chains into the corresponding human antibody expression vector were used. DNA fragments were co-incubated for ligation with T4 DNA ligase (New England Biolabs) at room temperature (RT) for 30 min and subsequently transformed with DH5α competent cells (Invitrogen) for plasmid isolation. To test if the ligation reaction formed the desired DNA sequence, a colony polymerase chain reaction (PCR) was performed. To this end, 0.2 µL of Taq DNA polymerase, 0.4 µL dNTPs (10 mM), 2 µL of 10x Taq buffer, as well as the forward and reverse primer were initially incubated at 94 °C for 5 min, followed by 25 cycles of 30 sec at 94 °C, 30 sec at 58 °C and 60 sec at 72 °C and finally 10 min at 72 °C. Chosen clones were purified by PCR clean up kit (Macherey Nagel) according to the manufacturer`s protocol and incubated in mini or maxi cultures overnight in Lysogeny Broth (LB) medium with 100 µg/mL ampicillin (Carl Roth) at 37 °C and 90 rpm. DNA was isolated the following day using Maxiprep (Thermo Fisher Scientific) or Miniprep kit (Qiagen) according to the provided protocol. DNA plasmids were also generated by Phusion PCR. Therefore, 4 µL of 5 x HF Buffer, 0.4 µL of 10 mM dNTP mix (Thermo Fisher Scientific), 0.2 µL of Phusion DNA polymerase (NEB) were incubated with the isolated DNA initially for 30 sec at 98 °C, 30 cycles for 10 sec at 98 °C, 20 sec at 60 °C and 15 sec at 71 °C, and finally for 7 min at 72 °C.

All plasmid concentrations were measured by a spectrophotometer (NanoDrop, Thermo Fisher) to quantify the amount of isolated DNA. Additionally, restriction digest and gel electrophoresis were used to visualize DNA with SYBR Safe DNA gel stain (Invitrogen). Sequence analysis (Eurofins Genomics) was used to control the gene sequence of each construct. Plasmids were stored at -20 °C until further use.

4.2.4. Antibody Production and Purification

Single chain antibodies and the respective full-length antibodies were produced by transient transfection of 293-6E cells. For antibody expression 0.45 µg/µL polyethylenimine (PEI) (Sigma Aldrich) was used as a transfection reagent. To this aim, sterile DNA was mixed with sodium chloride (150 mM), followed by slowly adding PEI and incubating the solution for 15 minutes at RT. Cells were cultured at 37 °C, 6% CO_2 in FreeStyle 293 Expression Medium. Seven days after transfection, culture supernatant containing secreted IgGs or scFvs was filtered through a 0.45 µm filter and purified using affinity chromatography with Protein G Sepharose (Sigma Aldrich). Protein G is genetically modified protein with three specific IgG binding regions and allows binding to the Fc part of most immunoglobulins and is therefore used for purification. Following this, antibodies were eluted with 0.1 M glycine (pH=3.0) in pre-filled tubes containing Tris hydrochloric acid (pH=8.0) for buffering.
Antibodies and scFvs were washed and concentrated in 1x PBS using Amicon Ultra-15 tubes (Merck Millipore) for buffer exchange and sterile filtrated in 0.22 µm Ultrafree-MC columns (Merck Millipore). Finally, antibody concentrations were determined and measured by a spectrophotometer (NanoDrop, Thermo Fisher). Additionally, correct antibody expression was checked by gel electrophoresis (SDS PAGE) performed according to the manufacturers protocol. Antibodies were stored in 1.5 mL tubes (Eppendorf) at 4 °C until further use.

4.2.5. HIV-1 Envelope Protein Production

293-6E cells were transfected for production of $YU2_{gp140}$ (fold-on trimer)[150] with PEI and incubated for seven days at 37 °C, 6% CO_2 shaking at 90-120 rpm. Culture supernatant was harvested and filtered through Ni-NTA agarose beads (Macherey-Nagel). After elution, buffer was exchanged using Amicon Ultra-15 100 kDa tubes with phosphate-buffered saline (PBS). Protein was stored at -80 °C.

4.2.6. HIV-1-Env ELISA

High-binding ELISA plates (Corning) were coated with 4 µg/mL of soluble HIV-Env, $YU2_{gp140}$ and were stored at 4 °C in a cold room overnight. This was followed by blocking the wells for 120 min at RT with 2% bovine serum albumin (BSA, Sigma Aldrich), 1 µM ethylenediaminetetraacetic acid (EDTA, Thermo Fisher), 0.1% Tween-20 in 1x PBS. Primary antibody concentration was adjusted to 68 nM, followed by a 1:4 dilution series and incubation for 90 min at RT. The secondary antibody, a horseradish peroxidase (HRP)-conjugated goat

anti-human IgG was diluted 1:1.000 in blocking buffer and incubated for 90 min at RT. For revelation of ELISA, ABTS solution (Thermo Fisher) was used, and absorbance was measured using a microplate reader (Tecan) at 405 nm plus reference wavelength at 695 nm. Between each step, plates were washed with PBS and 0.05% Tween-20. Samples were run in triplicates.

4.2.7. Cell Surface Binding

Antibody binding was also tested against cell surface expressed HIV-1-Env on HEK293T cells. For this reason, HEK293T cells were transfected either with $YU2_{gp140}$ or BaL_{gp140} using 2.5 M $CaCl_2$ and 2x HEPES buffered saline (HBS). After 48 h, transfected cells were washed in PBS and detached with cell dissociation buffer (Gibco). To evaluate the binding activity a fluorescence-activated cell scanning (FACS) analysis was performed. To this aim, primary antibodies were pre-diluted to 68 nM in PBS and incubated with the previously detached HEK293T cells. Samples were washed in 200 µL FACS Buffer (2µM EDTA, 2% FBS in 1x PBS), followed by incubation with goat anti-human IgG (1:5.000) (Biozol) and DAPI (1:100) (Invitrogen) for live-dead discrimination of analyzed cells. Following this, acquired data were analyzed with FlowJo software and the median fluorescence intensity (MFI) was determined to evaluate the binding between the antibodies and the cell surface expressed antigen.

4.2.8. Half-Life Determination in Non-Humanized Mice

Five full-length antibodies (IgG1 and IgG4) and the respective scFv-IgG4 were compared for their *in vivo* half-life in non-humanized NOD-$Rag1^{null}IL2rg^{null}$ mice. Different bNAbs were chosen based on their binding epitope: NIH45-46, 8ANC195, PGT145, 1-79 and 10E8. A total of 45 mice were included in the experiment. Each group contained 3 mice, and all were female. At the time of the experiment, mice were about six months old. For baseline values, mice were bled by puncture of Vena facialis (50 µL) a week before antibody injection. Following this, 200 µg of antibody was injected intravenously in the tail vein. During the injection, mice were kept in a restrainer as short as possible and were not under anesthesia. Subsequently, blood was collected at day 1, 3, 5, 8 and 11 after antibody injection in serum tubes (Sarstedt). Samples were stored for further analysis at -20 °C. Antibody serum levels were determined by performing a human IgG ELISA. Plates were coated with goat anti-human IgG (Jackson Laboratories) and incubated overnight at RT. Wells were blocked with blocking buffer (2% BSA, 1 µM EDTA, 0.1% Tween-20 in 1x PBS) for 1 h. Mice sera were diluted 1:20 in 1 x PBS and applied in a 1:3 dilution series. 1-79 scFv, IgG4 and IgG1 antibodies were used as a

standard antibody at a final concentration of 2 µg/mL. Followed by 90 min incubation at RT. Finally, an HRP-conjugated goat anti-human IgG (Jackson Laboratories) (1:1.000 diluted in blocking buffer) was applied to each well. Between each step, plates were washed with 0.05% Tween-20 in 1x PBS. ABTS solution (150 µL) was applied to each well and after four minutes, 100 µL of 1% SDS (sodium dodecyl sulfate) solution was added to stop the reaction. Immediately after that, absorbance was measured with an ELISA reader (Tecan). Antibody concentrations were determined by correlation to the curve of the standard antibody. The t1/2 was calculated as ln(2)/*K* with *K* as the rate constant, which is reciprocal to the X axis time units using one-phase decay in GraphPad Prism software.

4.2.9. HEp-2 Cell Immunofluorescence Assay

A clinically validated HEp-2 cell Immunofluorescence assay (NOVA Lite Hep-2 ANA Kit, Inova) was used to test antibodies for autoreactive behavior and was performed according to the manufacturer`s protocol. HEp-2 cells are originally derived from human laryngeal cancer, but furthermore it could be shown, that these cells are derivatives from HeLa cells[151]. These cells can be used as a nuclear substrate to detect antinuclear antibodies (ANAs), which play an important role in the diagnosis of autoimmune diseases[152,153].
To this aim, antibodies were pre-diluted to 1 µM in 30 µL PBS. After incubation and washing of plates, a fluorescein isothiocyanate (FITC) conjugated secondary anti-human IgG was added to detect a possible binding of antibodies to the nuclear substrates. All antibodies were applied in triplicate. A fluorescence microscope (DMI 6000 B from Leica) was used to acquire images with 200 ms exposure, 100 % intensity and gain 10. As a quality control a positive and negative control serum, supplied by the manufacturer, were tested at the same time. Results were assessed based on a positive or negative fluorescence in the nucleus.

4.2.10. Neutralization Assay

To compare the neutralization activity of scFv constructs and full-length antibodies a TZM.bl assay was performed. A dilution-series of antibodies was incubated with four different strains of HIV-1-Env-pseudoviruses and a control virus (BaL, YU2, Tro11, 25710 and MuLV). After 1 h, TZM.bl cells were added at a concentration of 10^4 per well. Furthermore, each plate contained a set of eight wells with cells only (background control) and another set with cells plus pseudovirus (virus control) and plates were incubated for 48 h at 37 °C and 5% CO_2. For enhanced infectivity, DEAE (diethylaminoethyl)-Dextran (Sigma Aldrich) was supplemented at 10 µg/mL into the medium. Following this, 150 µL of supernatant was removed and 100 µL of

luciferase reagent was added to each well. After 2 min incubation, 150 µL of cell/luciferase mix was transferred to a flat black 96-well microtiter plate (Sigma Aldrich). Plates were read in a luminometer, and luciferase activity was quantified by measuring the luminescence and relative luminescence units (RLU). Additionally, the 80% and 50% inhibitory concentrations (IC_{80} and IC_{50}) of the samples were subsequently determined by comparing the reduction of RLU to the RLU of virus control wells including the subtraction of background RLU of cell control wells[154].

4.2.11. Humanization of NOD-Rag1^{null}IL2rg^{null} (NRG) Mice

In order to infect mice with HIV-1, one to six-day old NRG mice were irradiated with up to 3.6 Gy of X-ray (MultiRad160) and were reconstituted with $CD34^+$ hematopoietic stem cells (HSC) after four to six hours of radiation (Figure 3). These HSCs were purified in 25 µL DMEM medium and in total $2x10^5$ cells were injected intrahepatically. To this aim, mice were manually fixed without narcosis. Hematopoietic stem cells were previously isolated with CD34 beads (Miltenyi Biotec) from cord blood and human placenta tissue as part of another project, and stored at -150 °C. The protocol of HSC isolation from cord blood and placenta tissue was approved by the Institutional Review Board of the University of Cologne (16-110) and donors provided written informed consent[85]. Three months after irradiation and injection of HSC, mice were tested for success of humanization. Therefore, 50 µL of blood was collected by puncture of the Vena facialis and samples were analyzed by flow cytometry to determine the level of chimerism. To this aim, the collected samples were stained with anti-mouse CD45-PE/Cy7 (BioLegend), anti-human CD45-Pacific Orange (Thermo Fisher), CD19-APC (BD), CD3-Pacific Blue (BD), CD4-PE (BD), CD8-FITC (BD) and CD16-AF700 (BD) for 30 minutes at 4 °C[85,155]. For determination of absolute cell numbers, counting beads (Thermo Fisher) were added. Data were finally analyzed by using FlowJo software. In addition, the successfully humanized mice were prepared for further experiments, particularly to test bNAbs in HIV-1 infected humanized mice. The experiments are explained in the following publication by Schoofs et al[156]. Further experiments were beyond this doctoral thesis.

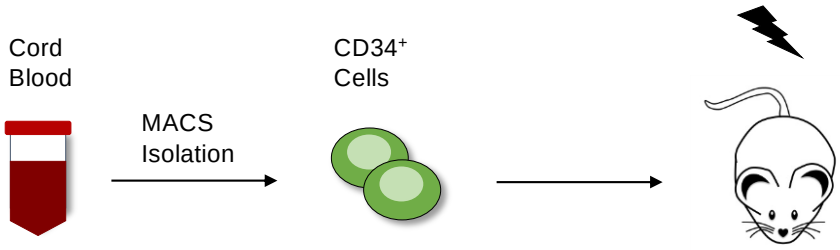

Figure 3: Humanization of NOD-Rag1^{null}IL2rg^{null} (NRG) mice.

CD34^{+} HSC are isolated from human cord blood and placenta tissue by MACS isolation. Within six days after birth, mice are irridiated with X-ray and four to six hours after irradiation, CD34^{+} stem cells are injected intrahepatically.

4.2.12. Statistical Analysis

Prism (GraphPad) Version 9 for MacOS was used for statistical analysis. FlowJo software was used to determine the mean fluorescence intensity (MFI) to evaluate the binding to cell surface expressed antigen between the different antibody classes. To compare the different antibody classes, MFI values were normalized on NIH4546 IgG1.

Neutralization data were acquired from CATNAP database[157], 80% and 50% inhibitory concentrations (IC_{50} and IC_{80}) were calculated by comparing the reduction of RLU to the RLU of virus control wells including the subtraction of background RLU of cell control wells as described in the method details. To check the success of the humanization, the arithmetic mean value of all humanized mice was calculated.

5. Results

5.1 Generation of Plasmid Constructs and Antibody Production

To compare scFv constructs based on bNAbs with their full-length IgGs regarding amongst others the binding behavior as well as the neutralization activity, sequences of already known anti-HIV-1 neutralizing antibodies were selected that bind different HIV epitopes. Included are the sequences of nine broad neutralizing antibodies and one neutralizing antibody: 10-1074, 3BNC117, PGT145, PGDM1400, NIH45-46, 4E10, 10E8, 8ANC195, 3BC176 and 1-79. In addition, two further constructs were created. The surface protein sCD4 and BW431/26, a humanized anti-CEA scFv, as a negative control[147].

All gene sequences were analyzed and compared with published sequences using MacVector and EXPASy ProtParam tool (https://web.expasy.org/protparam/), as well as IgBlast tool (https://www.ncbi.nlm.nih.gov/igblast/) on the World Wide Web. The results revealed that all antibody sequences were appropriately assembled. The variable light and heavy chain were correctly rearranged. Furthermore, the DNA quantity was determined by spectrophotometry at 260 nm, additionally plasmids could be detected by gel electrophoresis.

The plasmids were then used to produce antibodies for further analysis. Successful antibody expression could be observed on SDS-polyacrylamide gels (Figure 5). In non-reduced conditions, several bands could be observed for the full-length antibodies with the clearest band being greater than 250 kDa. For scFv constructs only one band at approximately 130 kDa could be assessed. In reduced conditions, scFv bands appeared at approximately 55 kDa and full length IgGs showed two bands at 25 kDa and 55 kDa. Finally, we used a spectrophotometer to quantify the concentration of produced antibodies at an absorbance of 280 nm. The total amount of all antibodies produced was between 0.07 mg and 5 mg. The final concentrations of the scFv constructs varied between 0.02 mg/mL and 6 mg/mL, for IgG4 between 0.35 mg/mL and 11.5 mg/mL and for IgG1 between 1.0 mg/mL and 25.6 mg/mL. The eluted volume varied between 0.05 mL and 1 mL and was comparable for all antibody classes. In conclusion, the measured concentrations of scFv constructs were lower than that of the IgGs despite the same transfection volume and the same procedure (Figure 6). Overall, the concentration of scFvs was 5 to 10-fold lower.

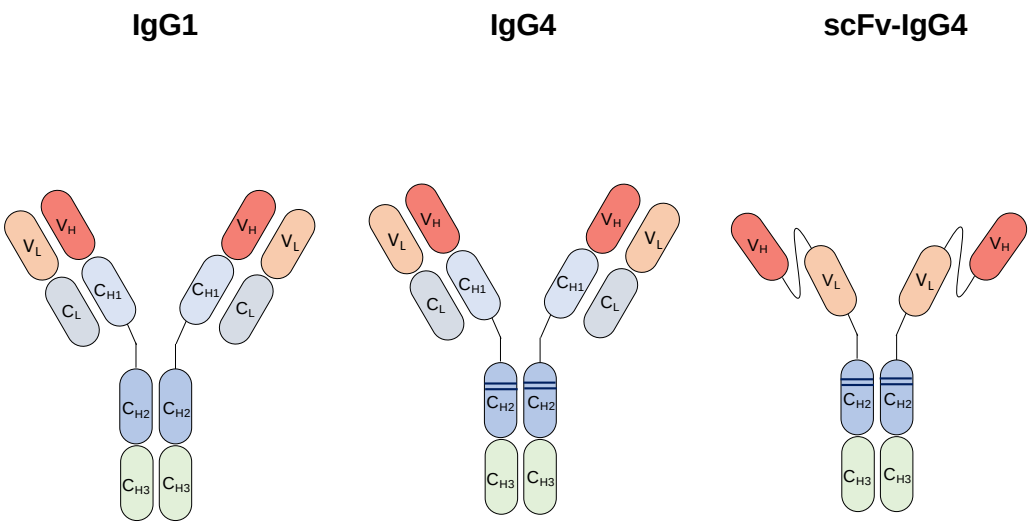

Figure 4: Three different antibody classes.

Shown are three different antibody classes, the variable light and heavy chain will be different for each chosen antibody. IgG4 and scFv IgG4 contains mutations shown as blue stripes for stabilizing the hinge region as well as for a reduced FcR binding and prolonged half-life. scFv IgG4 antibodies only contain the variable light and heavy chain of each chosen bNAb.

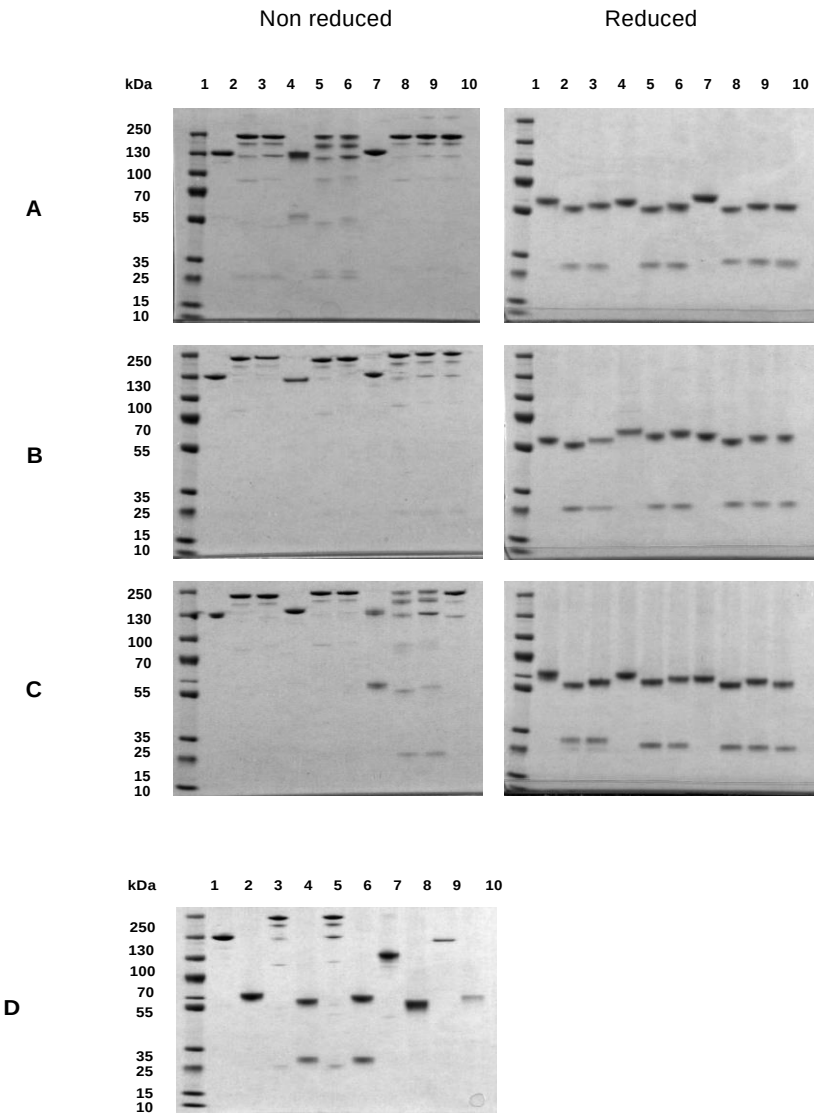

Figure 5: Successful antibody expression confirmed by SDS PAGE.

Antibodies are shown in unreduced and reduced conditions. Ladder on the right representing the molecular weight (kDa). **(A):** Lanes 1 to 10: 1-79 scFv IgG4, 1-79 IgG4, 1-79 IgG1, 3BC176 scFv IgG4, 3BC176 IgG4, 3BC176 IgG1, 3BNC117 scFv IgG4, 3BNC117 IgG4, 3BNC117 IgG1; **(B):** Lanes 1 to 10: 4e10 scFv IgG4, 4e10 IgG4, 4e10 IgG1, 8ANC195 scFv IgG4, 8ANC195 IgG4, 8ANC195 IgG1, 10-1074 scFv IgG4, 10-1074 IgG4, 10-1074 IgG1; **(C)**: Lanes 1 to 10: NIH4546 scFv IgG4, NIH4546 IgG4, NIH4546 IgG1, PGDM1400 scFv IgG4, PGDM1400 IgG4, PGDM1400 IgG1, PGT145 scFv IgG4, PGT145 IgG4, PGT145 IgG1, mGO IgG1; **(D):** Lanes 1 to 10: 10E8 scFv IgG4 unreduced, 10E8 scFv IgG4 reduced, 10E8 IgG4 unreduced, 10E8 IgG4 reduced, 10E8 IgG1 unreduced, 10E8 IgG1 reduced, CD4 unreduced, CD4 reduced, BW431/26 unreduced, BW431/26 reduced.

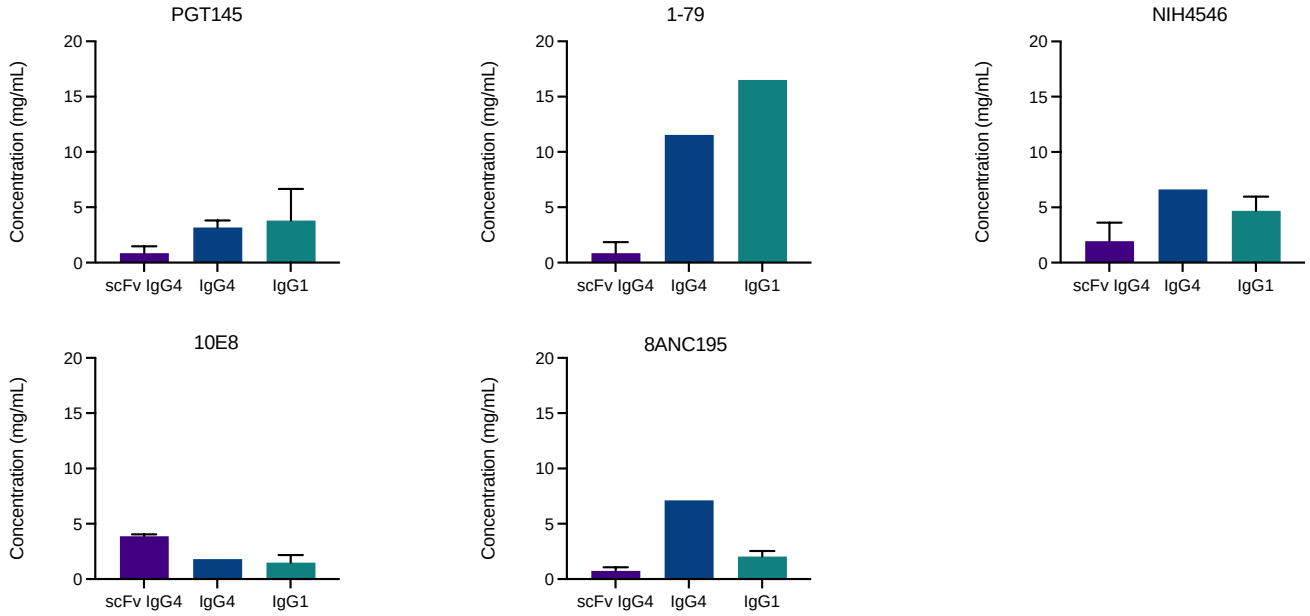

Figure 6: Comparison of antibody concentrations of five different bNAbs.

Shown are bar graphs of five anti-HIV-1 antibodies, which were used for *in vivo* application in non-humanized NRG mice. Graphs were created with Prism (GraphPad) to compare the final concentration of the respective antibodies. The bars represent the deviation of the different concentrations of the respective antibody production. The measured concentration of produced IgG1 and IgG4 full-length antibodies are higher compared to the concentration of scFv constructs. Most of the antibodies were produced multiple times.

5.2 HIV-1 Envelope Protein Production

After seven days of culturing, the His-tagged HIV Env protein $YU2_{gp140}$ (fold-on trimer)[150,158] was successfully eluted and purified by Ni-NTA affinity chromatography. A total of six elution steps were applied to SDS-polyacrylamide gels and clear bands matching to the glycoprotein could be detected only in the first three eluates

Figure 7). The concentration in eluates four to six varied between 0.0 mg/mL to 0.063 mg/mL. Following this, the first three eluates with a concentration between 0.406 mg/mL and 1.932 mg/mL were pooled. The final concentrated protein showed a distinct band at 140 kDa in reduced conditions with a total concentration of 6.12 mg/mL measured by spectrophotometry.

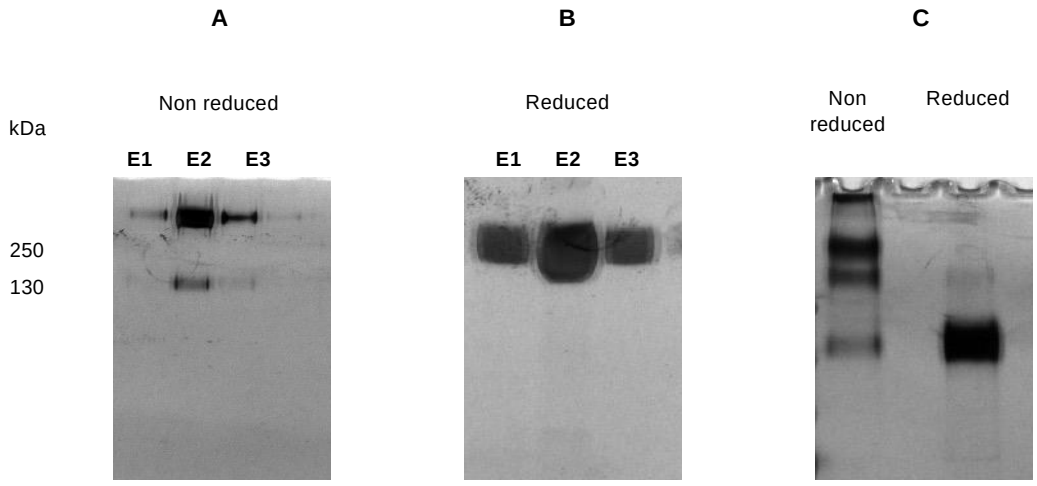

Figure 7: Expression of eluted envelope protein YU2gp140 after purification with Ni-NTA beads.

Silver stained SDS-polyacrylamide gel showed successful protein expression in the first three elution steps. Ladder on the right representing the molecular weight (kDa). **(A):** Elution one to three in non-reduced conditions. **(B):** Eluates under reduced conditions. **(C)**: Eluates containing a detectable signal were pooled and protein was concentrated, and successful expression was confirmed on SDS-polyacrylamide gel.

5.3 HIV-1-Env ELISA

Antibody constructs, which bind to different epitopes on the Env glycoprotein, were tested for their binding against a soluble trimeric glycoprotein ($YU2_{gp140}$) in an ELISA. The results showed, that 10-1074, 3BNC117 and NIH4546 antibodies achieved the highest OD values. These antibodies are characterized by binding to the CD4 binding site, which is fully represented in the fold-on trimer. In comparison to that, 8ANC195 or 4E10[159,160], binding to the gp120/41 interface or MPER (membrane proximal external region), showed a weak binding to the envelope protein. The BW431/26 control scFv did not recognize the HIV antigen as expected. Serial dilutions revealed that scFvs obtained a lower half-maximal effective concentration (EC_{50}) value than their parent antibody (Figure 8). The measured values were in general four to five-fold lower than that of the full-length antibody. However, this observation could not be made for 1-79, since the scFv antibody achieved similar values compared to 1-79 IgG1 and IgG4.

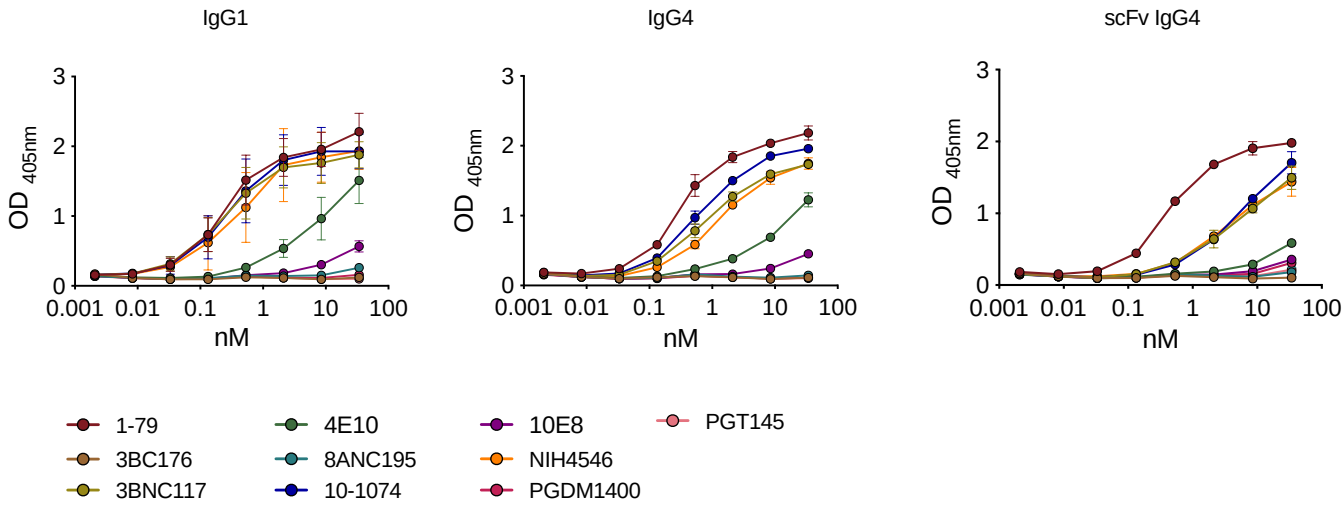

Figure 8: Antibodies tested in an ELISA against soluble $YU2_{gp140}$.

ELISA curves were created with Prism (GraphPad) to determine the half-maximal effective concentration (EC_{50}). The left y-axis shows the OD at 405 nm, and right x-axis shows concentration of antibody in nM. Graphs show mean and standard deviation represented by error bars of the respective antibodies, which are represented in different colors.

5.4 Cell Surface Binding

The HIV-1 envelope protein is composed of an extracellular located gp120 and a transmembrane protein gp41, building a trimeric spike[161]. To test how the scFv constructs, in comparison to the full-length IgGs, interact with the fully expressed envelope protein on the cell surface, which would be the target structure of CAR T cells, we transfected HEK293 T cells with different Env constructs $YU2_{gp140}$, BaL_{gp140} or an Env deficient control plasmid (PMX) (Figure 9). The transfection efficiency as well as the HEK293 T cell-antibody complex were quantified by flow cytometry analysis. Successfully transfected HEK293T cells expressed mCherry and the transfection efficiency varied between 35 to 40%. HEK293 T cells transfected with the Env-deficient control plasmid showed no expression. To visualize the binding between antibodies and envelope expressing cells, the mean fluorescence intensity (MFI) was determined after staining with a fluorescence conjugated goat anti-human IgG. The MFI values differed mainly between the two different HIV-1 strains, $YU2_{gp140}$ and BaL_{gp140}, for example 8ANC195 showed no binding against BaL_{gp140} transfected HEK293 T cells at all (Figure 10, Figure 11). However, the MFI was overall similar between scFvs and their parent antibodies showing that all antibody classes could bind to the glycoprotein. Furthermore, for 1-79, MFI values of the scFv construct was equal to the values of full-length IgGs. All MFI values were normalized for all antibodies to NIH4546.

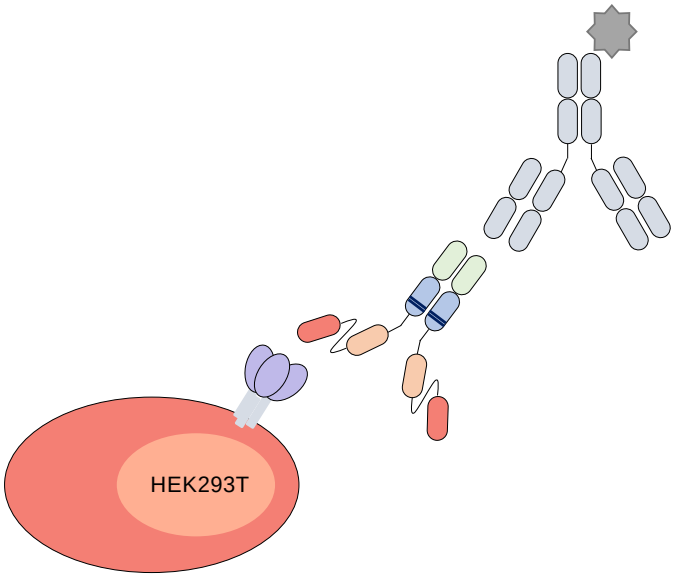

Figure 9: Binding between cell surface expressed $YU2_{gp140}$ and BaL_{gp140} and antibodies. Successfully transfected HEK293 T cell expressing mCherry with the envelope protein (either $YU2_{gp140}$ or BaL_{gp140}) on its cell surface is recognized by a scFv IgG4 antibody. During flow cytometry analysis this complex will be visible through a fluorescence conjugated goat anti-human IgG.

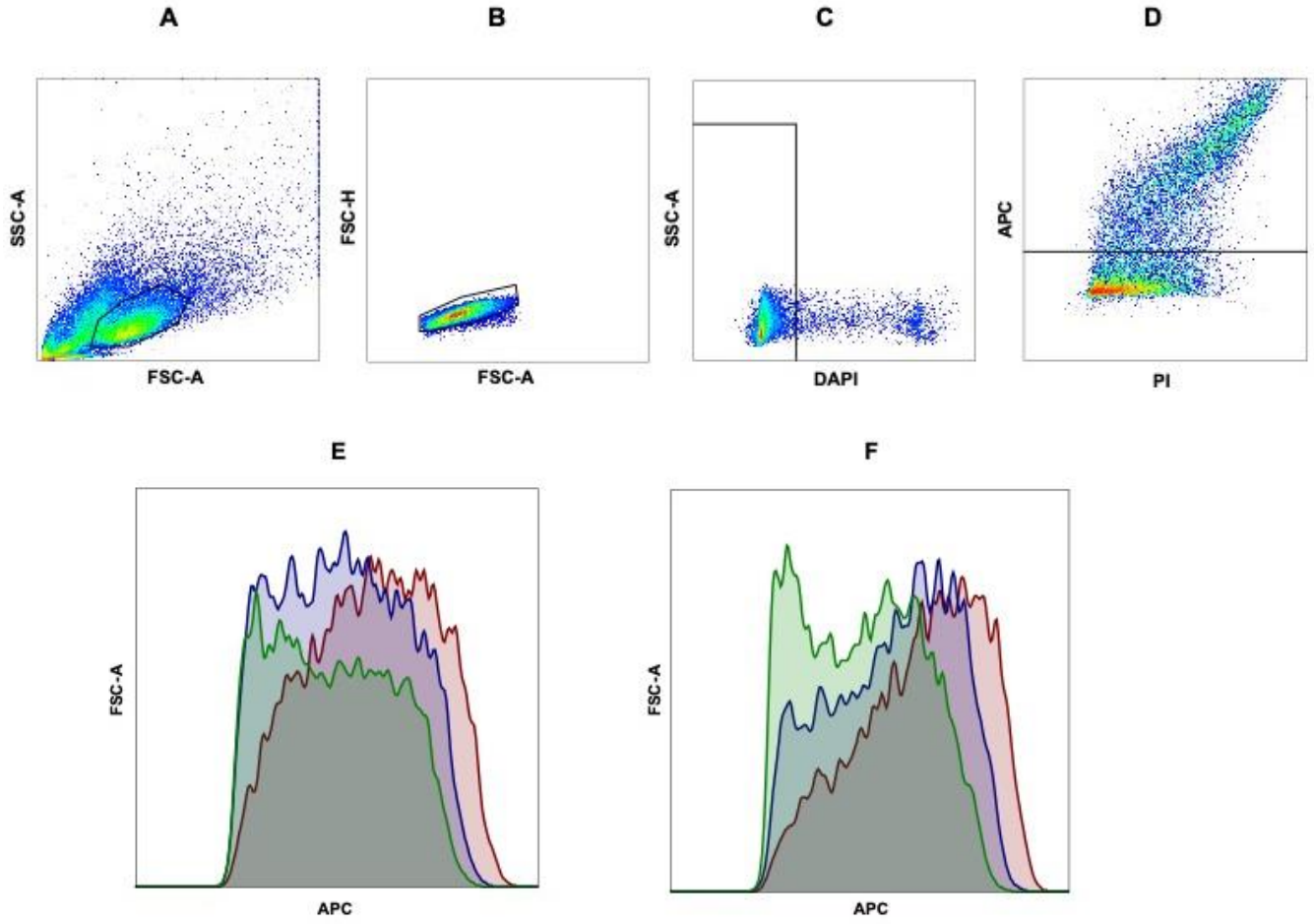

Figure 10: Gating strategy for FACS analysis of NIH4546 IgG1 against BaL_{gp140} (A-D) and overlay plot of NIH4546 against $YU2_{gp140}$ and BaL_{gp140} (E, F).

(A) and **(B)** showing the gate which includes population of HEK293 T cells which express BaL_{gp140} on the cell surface. **(C)**: Cells were stained with DAPI to differentiate live and dead cells. **(D)**: NIH4546 IgG1 binds to successfully transfected HEK293 T cells, this binding is visualized by the fluorescence conjugated goat anti-human IgG. **(E)**: Overlay plot of the MFI to visualize the binding between NIH4546 IgG1 (red), NIH4546 IgG4 (blue) and NIH4546 scFv IgG4 against against BaL_{gp140} expressing HEK293 T cells. **(F)**: Overlay plot of NIH4546 IgG1 (red), NIH4546 IgG4 (blue), NIH4546 scFv IgG4 (green) against $YU2_{gp140}$.

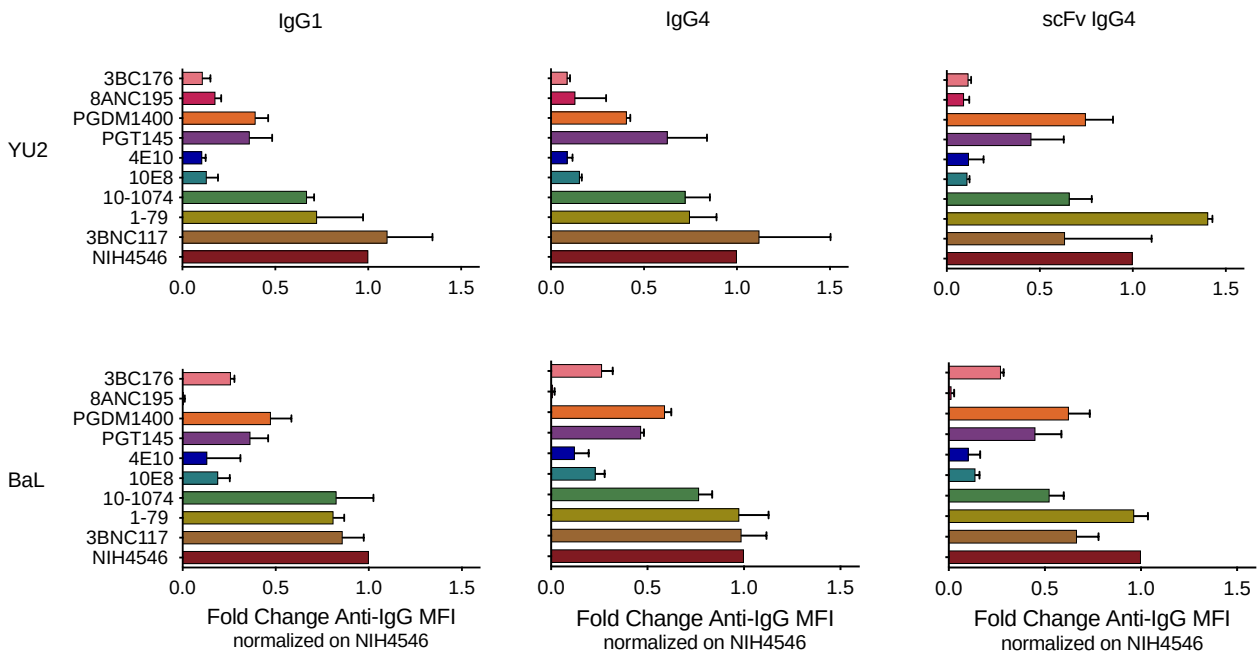

Figure 11: Scale bars representing fold change of MFI normalized on NIH4546.

Scale bars of each tested antibody against HEK293 T cells expressing either BaL_{gp140} or $YU2_{gp140}$. Bars representing the fold change of MFI with values normalized on NIH4546. Standard deviation is represented by error bars.

5.5 Half-Life Determination in Non-Humanized Mice

The scFv constructs, as well as the IgG4 full-length antibodies were constructed with a modified human IgG4 region. The missense mutations were introduced to stabilize the hinge region and to reduce Fc-binding to prolong the *in vivo* half -life. To confirm that these mutations compared to the unmodified IgG1 antibodies lead to longer in vivo persistence, five different broadly neutralizing antibodies were selected for half-life analysis in non-humanized NRG mice. Each one of them targets a different epitope on the HIV-1 envelope glycoprotein: NIH45-46 (CD4bs), 10E8 (MPER), PGT145 (V1/V2 loop), 1-79 (V2/V3 loop) and 8ANC195 (gp120/gp41 interface). Serum samples were collected on different time points to determine the antibody concentrations by total IgG enzyme-linked immunosorbent assay (ELISA)[85]. Half-life was determined by calculation of the mean. The results showed that scFv and IgG4 antibodies achieved longer half-lives compared to the corresponding IgG1 antibody (Figure 12). Additionally, it could be observed that the *in vivo* persistence of scFvs, IgG4s and IgG1s varied between the different bNAb groups. PGT145 and 1-79 achieved the longest half-life values. 1-79 IgG4 and scFv antibodies could still be detected 16.4 and 5.3 days after injection. In contrast, 1-79 IgG1 had a half-life of 2.7 days. 8ANC195 showed half-life values for scFv and IgG4 antibodies of 2.3 and 2.2 days. IgG1 only 0.74 days.

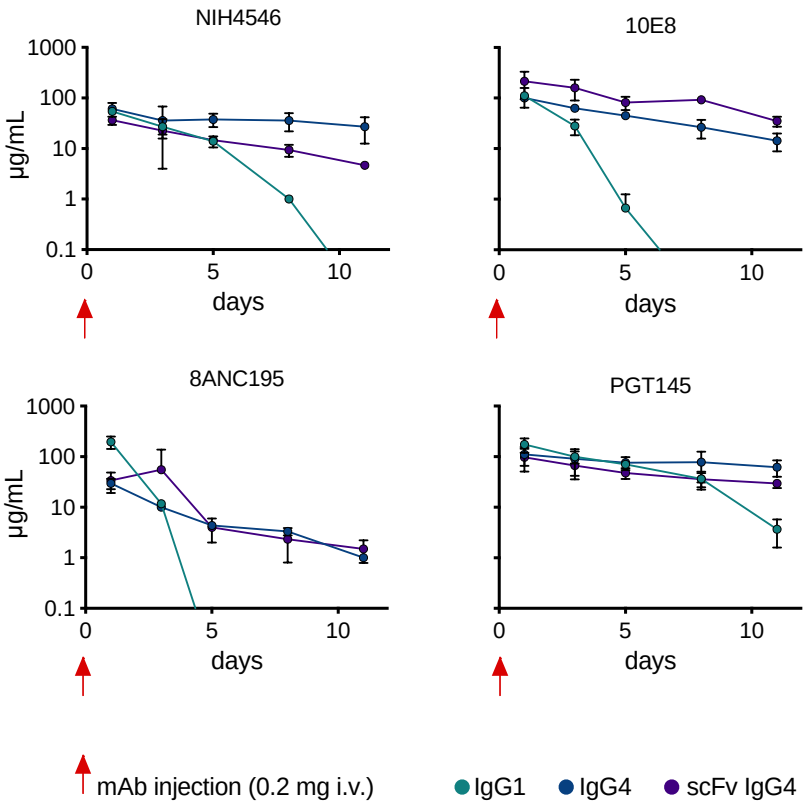

$t_{1/2}$ (days)	IgG1	IgG4	scFv IgG4
NIH4546	1.37	9.1	3.7
8ANC195	0.74	2.2	2.3
PGT145	2	16.8	7.2
1-79	2.7	16.4	5.3
10E8	1.4	3.9	5

Figure 12: *In vivo* application of five antibody constructs in non-humanized mice.

Graphs show serum levels of antibodies in non-humanized mice after intravenous injection of 0.2 mg of each antibody. Left y-axis show concentration in µg/mL, right x-axis show time in days. Lines indicate change of plasma levels. Data are calculated as mean with standard deviation. Table shows the calculated half-life in days of the individual antibodies.

5.6 HEp-2 Cell Immunofluorescence Assay

It is known that bNAbs can show autoreactive behavior[162]. Furthermore, the investigation of potential autoreactivity and polyreactivity is important since there might be an influence on half-life and the behavior of administered bNAbs *in vivo*. To investigate this, a clinically validated HEp-2 cell assay was performed. This indirect immunofluorescence assay is used regularly in everyday clinical practice to detect anti-nuclear antibodies (ANAs), which are important for the diagnosis of autoimmune diseases[152,153]. The visual representation of a potential binding of the bNAbs to the HEp-2 cells is achieved with a FITC conjugated antibody. The binding is visible as a green fluorescence.

For all applied scFvs and full-length antibodies, a green fluorescence could be observed (Figure 13). A high intensity achieved 4E10, 10E8 and NIH45-46. 4E10, a bNAb binding to the MPER, is long known for its polyreactive properties[163,164]. 1-79 scFv, IgG4 and IgG1 showed in comparison to the other bNAbs only a weak fluorescence signal. In general, an increase of the fluorescence of scFv constructs compared to their parent IgGs could not be observed. The binding pattern was broadly similar between the bNAbs and if IgG1 antibodies had shown reactivity, then the same was found for the other variants.

A

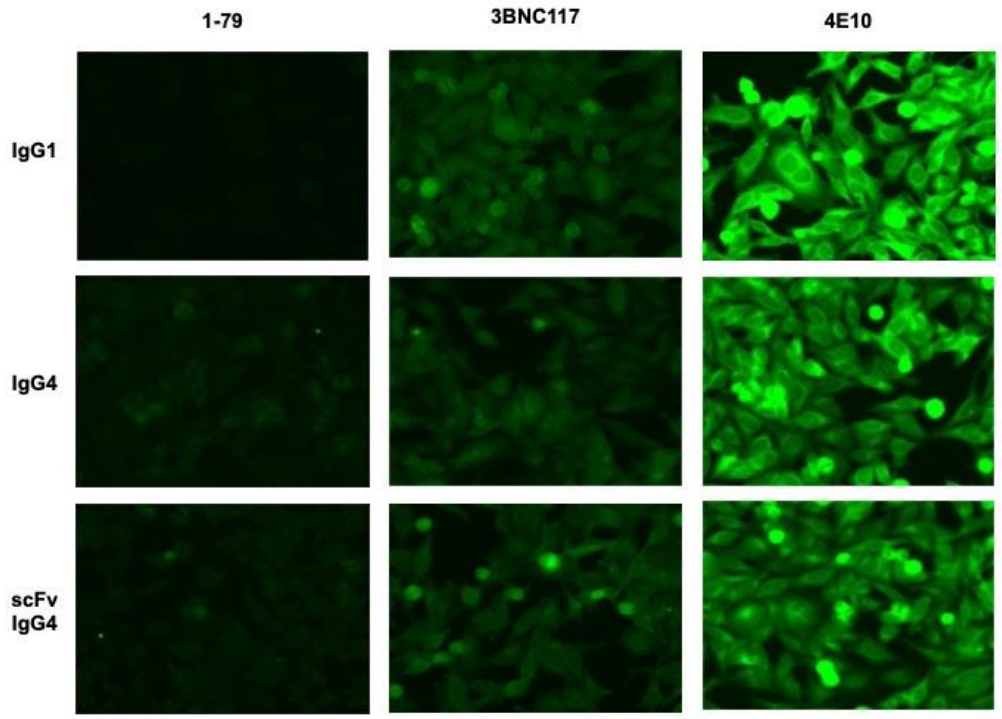

B

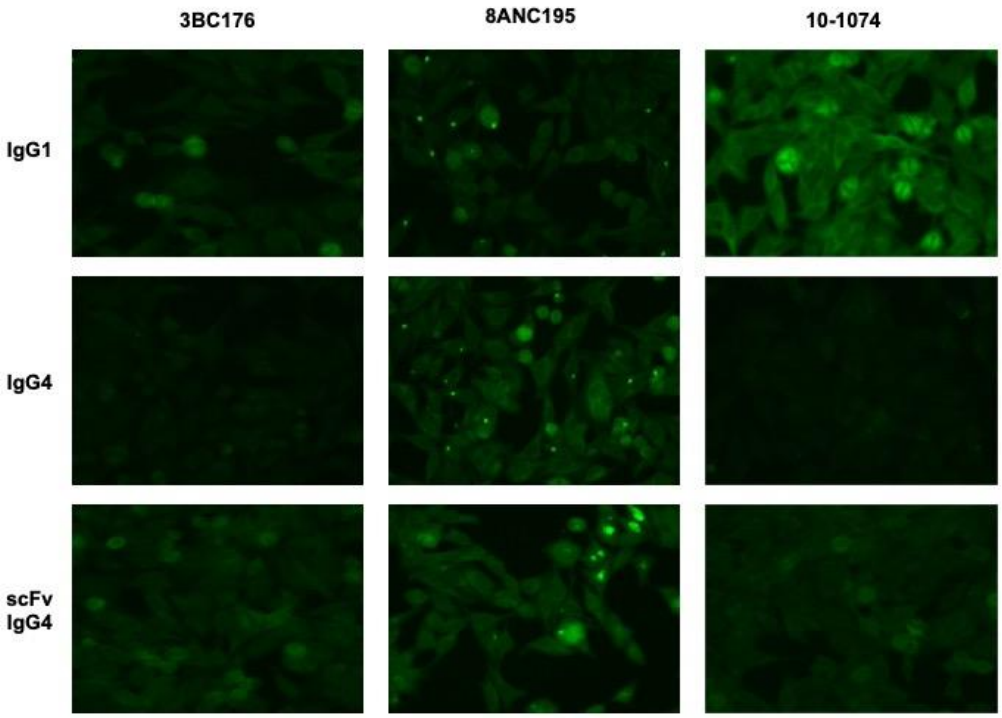
3BC176
8ANC195
10-1074
IgG1
IgG4
scFv
IgG4

C

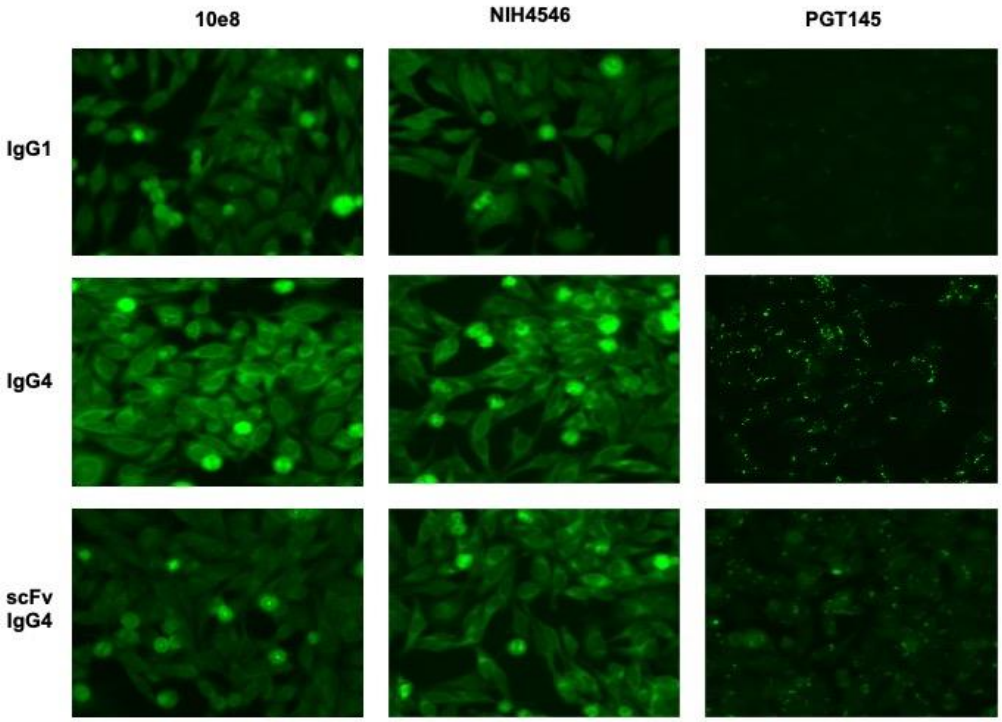
10e8
NIH4546
PGT145
IgG1
IgG4
scFv
IgG4

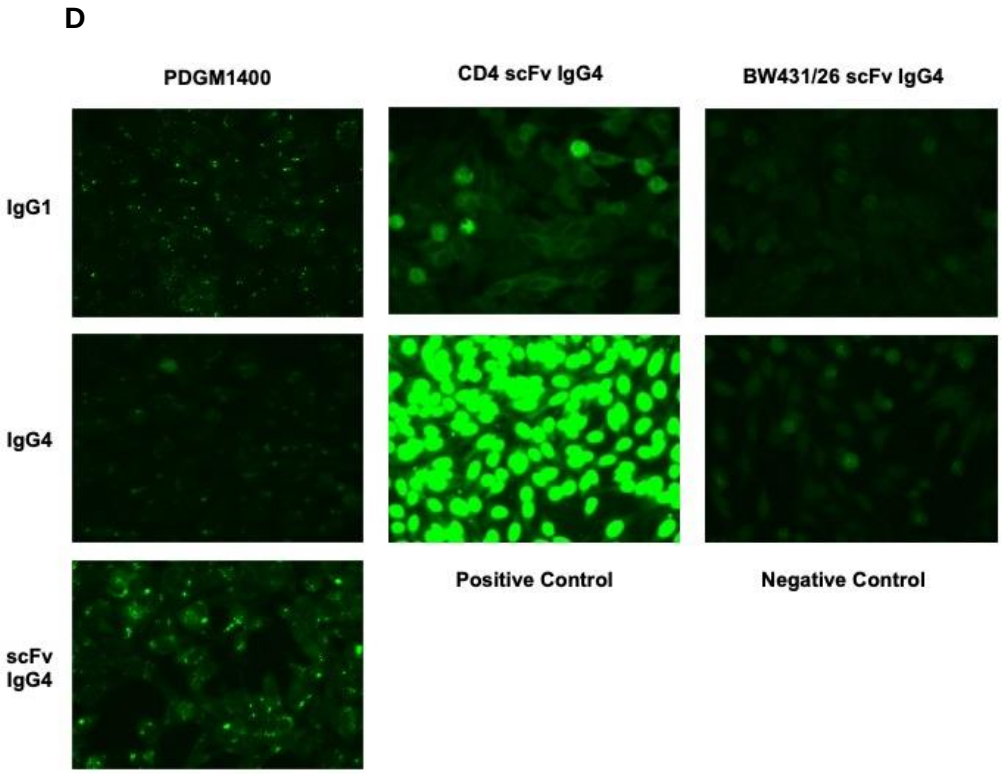

Figure 13: Evaluation of the polyreactivity in a clinical validated HEp-2 cell assay.

(A-D): Representative images shown. All antibody constructs were tested in a HEp-2 cell assay and tested for potential polyreactivity at a concentration of 1 µM. Furthermore, **(D)** includes positive and negative control provided by the manufacturer. Data were acquired in triplicates. Scale bar = 100 µm.

5.7 Antibody Neutralization Assay

A TZM-bl cell assay was used to investigate the neutralization activity of scFv antibodies and their activity compared to full-lengths antibodies[145,154]. To this end, all antibodies were tested for their ability to inhibit infection of a panel of four different HIV-1-Env-pseudoviruses: YU2, BaL, Tro11, 25710, as well as murine leukemia virus (MuLV) as a negative control[165]. Luciferase activity was measured and IC_{80} and IC_{50} (50% and 80% inhibitory concentration) values were determined. The results showed that 3BNC117 and 10-1074 IgG1 and IgG4 obtained a superior activity compared to the other bNAbs including the corresponding scFv construct against the four pseudoviruses. For example, the IC_{50} values for 3BNC117 IgG1 and IgG4 were found between 0.01 µg/mL and 0.34 µg/mL against all four pseudoviruses. These values confirm the results that have already been shown in previous publications[91,166]. 3BC176 and 4E10 antibodies showed the highest IC_{80} and IC_{50} values against all pseudoviruses. For example, 4E10 IgG1 showed IC_{50} values between 0.84 µg/mL and 12.75 µg/mL and 3BC176 IgG1 between 1.07 µg/mL and 2.84 µg/mL. In contrast, the IC_{50} values of the scFv constructs against all four pseudoviruses were above 17 µg/mL. Overall, the results show that higher concentrations of scFv are required compared their parent IgG (Table 2). The IC_{80}/IC_{50} values of scFv constructs were approximately one $\log_{10}$ higher compared to the corresponding IgGs. Whereas these results did not apply for 1-79 and PGT145. 1-79 scFv achieved similar values for the neutralization activity compared to its respective full-length IgGs with a geometric mean IC_{50} of 0.17 µg/mL to 0.3 µg/mL. For PGT145, a broadly neutralizing antibody that targets the apex of the HIV envelope trimer at the V1/V2 β sheets, similar results could be perceived. ScFv, IgG4 and IgG1 were able to neutralize pseudovirus 25710 with a geometric mean IC_{50} of 0.01 µg/mL to 0.03 µg/mL[78,167].

Table 2: Measured IC_{50} and IC_{80} values from TZM.bl assay.

A

µg/mL		YU2		BaL		Tro11		25710		MuLV	
		IC50	IC80	IC50	IC80	IC50	IC80	IC50	IC80	IC50	IC80
1-79	IgG1	>24	>24	0,26	0,88	24,92	24,92	24,92	24,92	24,92	24,92
	IgG4	>24	>24	0,17	0,66	24,92	24,92	24,92	24,92	24,92	24,92
	scFv	17,87	17,87	0,30	1,17	17,87	17,87	17,87	17,87	17,87	17,87
3BC176	IgG1	1,42	16,46	2,84	12,06	2,59	22,69	1,07	19,11	25,12	25,12
	IgG4	0,96	12,12	2,06	9,25	1,94	15,55	0,61	14,27	25,12	25,12
	scFv	18,02	18,02	18,02	18,02	18,02	18,02	18,02	18,02	18,02	18,02
3BNC117	IgG1	0,03	0,09	0,01	0,03	0,04	0,20	0,33	1,17	25,00	25,00
	IgG4	0,03	0,09	0,01	0,05	0,06	0,22	0,34	1,59	24,94	24,94
	scFv	0,20	0,60	0,17	0,73	0,47	1,51	17,77	17,77	17,77	17,77
4E10	IgG1	12,75	>24	6,08	24,97	1,58	9,51	0,84	4,19	24,97	24,97
	IgG4	19,33	>24	11,21	24,90	3,00	16,21	1,75	7,18	24,90	24,90
	scFv	17,73	17,73	17,73	17,73	17,73	17,73	17,73	17,73	17,73	17,73
8ANC195	IgG1	0,39	1,39	>24	25,23	0,14	0,52	0,79	3,39	25,23	25,23
	IgG4	0,48	1,73	>24	25,16	0,17	0,65	0,88	4,47	25,16	25,16
	scFv	11,49	17,99	17,99	17,99	1,81	6,09	17,99	17,99	17,99	17,99
10-1074	IgG1	0,15	0,46	0,03	0,10	0,02	0,07	0,08	0,26	25,28	25,28
	IgG4	0,13	0,41	0,03	0,10	0,02	0,06	0,08	0,23	25,21	25,21
	scFv	0,94	2,91	0,31	0,95	0,20	0,57	0,75	1,96	18,20	18,20
10E8	IgG1	0,91	4,61	0,39	2,18	0,05	0,31	0,04	0,23	25,17	25,17
	IgG4	1,21	6,00	0,50	2,63	0,06	0,44	0,04	0,25	25,11	25,11
	scFv	5,67	18,09	3,17	15,88	0,48	2,39	0,36	1,74	18,09	18,09
NIH4546	IgG1	0,02	0,07	0,01	0,05	0,76	4,60	0,24	0,92	25,10	25,10
	IgG4	0,03	0,09	0,02	0,07	1,31	8,12	0,31	1,14	25,04	25,04
	scFv	0,18	0,55	0,43	3,05	17,87	17,87	3,30	15,90	17,87	17,87
PGDM1400	IgG1	0,29	0,81	0,23	17,01	0,40	1,34	0,01	0,01	25,92	25,92
	IgG4	0,27	0,86	0,16	17,29	0,38	1,30	0,01	0,01	25,86	25,86
	scFv	0,77	2,73	1,14	18,69	1,02	3,15	0,01	0,02	18,69	18,69
PGT145	IgG1	0,08	0,23	23,48	25,82	0,07	0,19	0,01	0,03	25,82	25,82
	IgG4	0,06	0,16	11,02	25,76	0,06	0,17	0,01	0,03	25,76	25,76
	scFv	0,19	0,55	18,59	18,59	0,15	0,45	0,03	0,18	18,59	18,59

< 0,1 µg/mL
0,1 - 0,5 µg/mL
0,51 - 2,0 µg/mL
> 2,0 µg/mL

B

nM		YU2		BaL		Tro11		25710		MuLV	
		IC50	IC80	IC50	IC80	IC50	IC80	IC50	IC80	IC50	IC80
1-79	IgG1	>170	>170	1,79	6,00	>170	>170	>170	>170	>170	>170
	IgG4	>170	>170	1,14	4,49	>170	>170	>170	>170	>170	>170
	scFv	>170	>170	2,86	11,14	>170	>170	>170	>170	>170	>170
3BC176	IgG1	9,68	111,89	19,30	81,99	17,61	154,23	7,29	129,87	>170	>170
	IgG4	6,50	82,41	14,03	62,88	13,21	105,72	4,13	96,98	>170	>170
	scFv	>170	>170	>170	>170	>170	>170	>170	>170	>170	>170
3BNC117	IgG1	0,18	0,60	0,08	0,23	0,29	1,35	2,23	8,01	>170	>170
	IgG4	0,20	0,64	0,10	0,31	0,40	1,48	2,30	10,92	>170	>170
	scFv	1,91	5,76	1,64	7,05	4,52	14,48	>170	>170	>170	>170
4E10	IgG1	87,17	>170	41,57	>170	10,83	65,02	5,76	28,66	>170	>170
	IgG4	132,55	>170	76,87	>170	20,56	111,17	12,02	49,20	>170	>170
	scFv	>170	>170	>170	>170	>170	>170	>170	>170	>170	>170
8ANC195	IgG1	2,64	9,38	>170	>170	0,95	3,55	5,38	22,92	>170	>170
	IgG4	3,26	11,72	>170	>170	1,13	4,44	6,00	30,36	>170	>170
	scFv	109,03	>170	>170	>170	17,15	57,78	>170	>170	>170	>170
10-1074	IgG1	1,02	3,12	0,21	0,70	0,14	0,50	0,56	1,78	>170	>170
	IgG4	0,90	2,79	0,20	0,65	0,12	0,44	0,51	1,59	>170	>170
	scFv	8,81	27,29	2,95	8,94	1,83	5,30	7,00	18,35	>170	>170
10E8	IgG1	6,19	31,30	2,65	14,80	0,34	2,12	0,24	1,56	>170	>170
	IgG4	8,26	40,77	3,37	17,88	0,40	3,01	0,25	1,72	>170	>170
	scFv	53,54	>170	29,88	149,86	4,51	22,57	3,38	16,40	>170	>170
NIH4546	IgG1	0,16	0,50	0,10	0,36	5,19	31,30	1,64	6,27	>170	>170
	IgG4	0,21	0,63	0,13	0,47	8,95	55,35	2,11	7,79	>170	>170
	scFv	1,75	5,27	4,11	29,17	>170	>170	31,51	151,99	>170	>170
PGDM1400	IgG1	1,89	5,35	1,50	112,05	2,63	8,84	0,08	0,08	>170	>170
	IgG4	1,75	5,70	1,07	114,16	2,49	8,61	0,08	0,08	>170	>170
	scFv	7,07	24,92	10,43	>170	9,31	28,81	0,08	0,18	>170	>170
PGT145	IgG1	0,50	1,49	155,27	>170	0,43	1,23	0,08	0,23	>170	>170
	IgG4	0,38	1,09	73,05	>170	0,40	1,15	0,08	0,20	>170	>170
	scFv	1,79	5,07	>170	>170	1,36	4,16	0,30	1,68	>170	>170

< 1 nM
1.1 - 5 nM
5.1 - 20 nM
> 20 nM

Tables show the measured IC_{50} and IC_{80} values (A: in µg/mL, B: in nM) representing the neutralization activity of all antibody constructs which were tested against a panel of four pseudoviruses and a control pseudovirus (Murine Leukemia Virus) as a negative control. Neutralization testing was performed in duplicates at a concentration of 3.415 µM. Numbers are color-coded with values < 0.1 µg/mL and < 1 nM highlighted in red, between 0.1 µg/mL - 0.5 µg/mL and 1.1 nM - 5 nM in orange, 0.51 µg/mL - 2.0 µg/mL and 5.1 nM - 20 nM in yellow, > 2.0 µg/mL and > 20 nM in white.

5.8 Humanization of NOD-Rag1^{null}IL2rg^{null} Mice

Animal models are crucial for further investigation of antiretroviral therapies and their impact on the HIV-1 reservoir. It has already been shown that humanized mouse models are able to mimic the human immune system and allow further *in vivo* analysis of antibody constructs and anti-HIV-1 CAR T cells[142,143]. Therefore, a humanized mouse model was established and a systemic analysis of the humanization efficiency from placenta tissue and umbilical cord blood was carried out. NOD mice with a disruption in the recombinase activating gene 1 (*Rag1^{null}*) as well as in the interleukin receptor common gamma chain (IL-2rg^{null}), were reconstituted with hematopoietic stem cells isolated from placenta tissue[85]. In total, 322 mice were humanized for further experiments. Twelve weeks after CD34$^+$ HSC injection, mice were tested for engraftment with flow cytometry analysis (Figure 14). Percentage of human CD45$^+$ cells of total CD45$^+$ cells in peripheral blood varied between 0.015% and 82% (arithmetic mean 0.14%). Level of CD19$^+$ cells were found to be between 0% and 94.8% (arithmetic mean 0.4%). The proportion of CD3$^+$ cells was between 0% and 100% (arithmetic mean 0.24%). The CD3 subpopulations, CD4$^+$ and CD8$^+$ cells have been determined as well. Values for CD4$^+$ T cells were between 0% and 100% (arithmetic mean 0.5%) and for CD8$^+$ T cells between 0% and 100% (arithmetic mean 0.4%). Additionally, total numbers of CD4$^+$ T cells/µL were determined. Mice with at least one CD4$^+$ T cells/µL were chosen for further experiments. Therefore, selected mice contained between 1 to 6427 CD4$^+$ T cells/µL with an arithmetic mean of 41 CD4$^+$ T cells/µL. 107 of 322 tested mice had less than one CD4$^+$ T cells/µL and could not be used for further experiments.

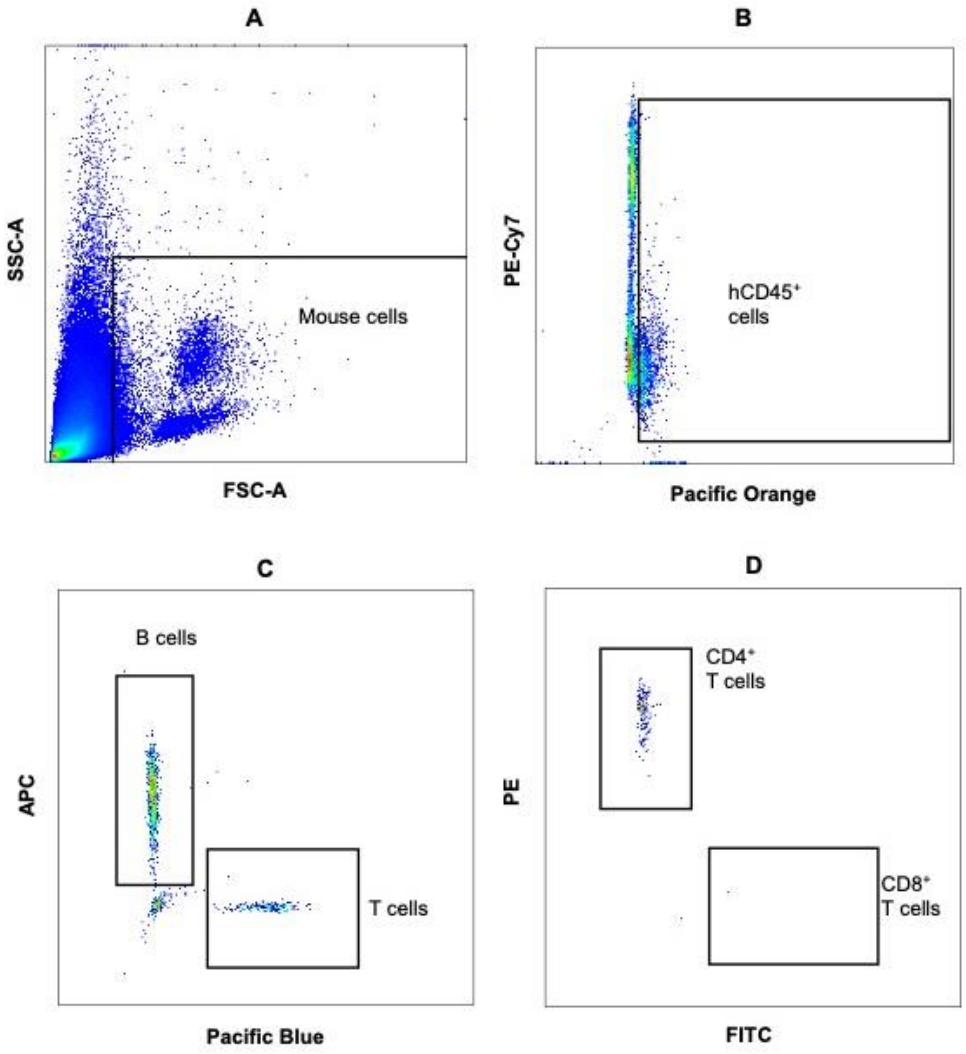

Figure 14: FACS dot plot exemplary for a successfully humanized mouse.

(A): Set gate containing all mouse cells, which are subsequently divided into human $CD45^+$ cells **(B)**. **(C)**: Human $CD45^+$ cells are further separated in $CD19^+$ B and $CD3^+$ T cells. **(D)**: CD3 population is divided in $CD4^+$ and $CD8^+$ T cells, which are necessary for HIV infection. FACS dot plots were created with FlowJo software.

6. Discussion

Despite plenty years of research, there is no cure for HIV-1 infection to this day. Antiretroviral medication can suppress viremia and allows a normal life expectancy, but a lifelong commitment and adverse effects often lead to incompliance. Prevention and therapy with broadly neutralizing antibodies are still under investigation, but clinical studies are promising. Nevertheless, establishment of a latent reservoir of the virus might be an obstacle to this therapy[42]. Immune therapies, e.g., CAR T cell therapy, in combination with latency reversing agents might be the only option to achieve a cure of HIV-1 infection[94,168,169]. However, the potency of LRAs and the occurrence of side effects still require improvement.

The discovery of potent bNAbs in the last two decades, offers new possibilities for anti-HIV-1 CAR design[78,85,93]. CAR T cells for HIV-1 treatment have been already developed several years ago but were abandoned due to lack of efficacy[130,170,171]. The recent identified antibodies offer the possibility of attacking structures other than CD4 as it was done initially. In the meantime, the application of CARs has made a big progress in treatment of hematological malignancies[103,134]. The binding domain of CARs is often composed of a single chain antibody. These antibodies, consisting out of the variable light and variable heavy chain of an antibody, can target every cell surface expressed protein, as well as carbohydrate and glycolipid structures, and therefore allowing to bind to a specific antigen[112,133,172]. Furthermore, the development of CAR design with new stimulatory and co-stimulatory domains makes this therapeutic approach more effective. The characterization of these scFvs based on bNAbs as a potential targeting domain of CARs is the main topic of this thesis.

In order to test new therapy approaches, it is important to have suitable *in vivo* models available to test their effectiveness and safety. Thus, an additional aspect of this thesis was focused on the establishment of a humanized mice model using placental tissue and cord blood derived stem cells.

6.1 Essential Properties of IgG1 Antibodies are retained as scFvs

To investigate the characteristics of scFvs, we cloned twelve different scFv constructs and compared these to the respective full-length IgG1s and IgG4s. These antibodies were selected to target different epitopes on the HIV-1 envelope glycoprotein.

First, we determined whether the binding behavior of scFvs remained comparable. Although scFvs are built by the variable light and heavy chain of an antibody, which are known to be responsible for the antigen recognition, they have conformational differences compared to full-length antibodies, which could influence the effectiveness. We expected that the produced scFv constructs achieve the same binding to the envelope protein compared to full length immunoglobulins[112]. The binding of antibodies was tested against soluble protein and cell

surface expressed protein, since we wanted to investigate how scFvs interact with the fully expressed envelope protein on the cell surface, which would be the target structure of CAR T cells. These tests revealed that the HIV-1-Env binding patterns of scFvs compared to their parent bNAb remained similar but higher quantities of scFvs are required (Figure 8; Figure 11). The mean fluorescence intensity (MFI) was determined to quantify the binding between antibodies and envelope expressing cells. The MFI describes the amount of bound fluorescent dye per particle. The results showed that MFIs of bNAbs varied between the HIV-1 strains, $YU2_{gp140}$ and BaL_{gp140}, meaning that some antibodies could bind $YU2_{gp140,}$ but not BaL_{gp140}. Additionally, scFvs presented in general lower MFI values compared to IgG1 and IgG4 constructs, which indicates a lower affinity of most of the scFv antibodies to the cell surface expressed protein. However, this could not be observed for 1-79 scFv, which showed comparable binding patterns as observed for the 1-79 IgG1 and IgG4 antibodies. Wang and colleagues showed that single chain antibodies obtain five-to-ten-fold lower antigen binding affinity than the respective full-length antibody[173,174]. Nevertheless, scFvs might remain enough affinity to be an optimal candidate for CARs, as there might be an affinity threshold to achieve optimal T cell effector function.

Broadly neutralizing antibodies are characterized by an unusually long heavy chain complementarity-determining region 3 (HCDR3) and high mutation rates in VDJ-genes. It has been shown that these properties can lead to polyspecificity and autoreactivity[162,163,175].

Furthermore, the conformational change of scFv constructs could additionally lead to increased auto-reactive properties. Therefore, we performed a HEp-2 cell immunofluorescence assay. We were unable to see an increase in the fluorescence intensity against the human epithelial cells for any of the constructs. However, differences in the fluorescence pattern for each antibody class could be observed under the microscope. These patterns were the same for the scFvs and their respective parent antibodies. The fluorescence intensity has not been quantified.

To investigate the neutralizing activity, scFvs and full-length immunoglobulins were compared in a TZM.bl cell assay. It could be observed that the potency to neutralize a panel of four pseudoviruses was less for almost all single chain antibodies. Interestingly, two bNAbs were found to make an exception. 1-79 and PGT145 achieved comparable values for the 50% and 80% inhibitory concentrations. Hale et al. already tested a PGT145-HIV-CAR *in vitro* and could show sufficient cytokine production and killing of HIV^{pos} target cells[70].

1-79 was originally found to be a non-broad neutralizing antibody and therefore only neutralizes a few HIV-1 strains[176]. This antibody binds the V3 loop of the envelope protein, which is not accessible in most HIV-1 isolates, as it is covered by the V1/V2 loop. On HIV-1 entry, the V3 loop is exposed because the interaction between CD4 and gp120 induces a conformational

change in the envelope[177,178]. It could be shown that it might be difficult for full-length antibodies to bind to the V3 loop, as the distance between the epitope and the cell membrane is estimated to be 45Å to 80Å, whereas the size of an immunoglobulin contains approximately 115Å. In contrast, the size of a scFv in its soluble form is estimated around 40Å, suggesting that some epitopes are more accessible to scFvs than IgGs and therefore achieve an efficient neutralizing activity[179,180]. Anti-V3 antibodies can be found in almost all HIV-1 infected persons and in addition to that, vaccinated V3 antibodies tested in individuals could reduce the rate of HIV-1 infections[178]. However, in the case of scFvs bound to CAR T cells, these findings cannot be simply applied since there are two cells involved. In addition, the neutralization activity, which is crucial for soluble antibodies, is not a decisive criterion for antibodies bound to CAR T cells since it attacks the target cell through its cytotoxic properties.

6.2 Extended Half-Life of scFv *in vivo* and Establishment of a Humanized Mouse Model

Furthermore, we injected scFvs and IgGs intravenously in non-humanized mice, compared the in vivo persistence, and determined the half-life. When CAR T cells are administered in an ART pretreated *in vivo* model with no antigen burden, it should be considered that low levels could cause a missing expansion of CAR T cells. The goal is therefore to achieve a long half-life of the antibodies through mutations in the constant IgG4 region. The measured antibody plasma concentrations indicated that scFv-IgG4 and IgG4 antibodies exhibited longer half-lives than the IgG1 constructs, which means that the mutations support the persistence of the soluble scFv-IgG4 and IgG4 antibodies[119,149]. However, this does not mean that these mutations will have the same effect in CAR T cells, but it might support it. Further investigation is required.

Humanized mouse models can mimic the human immune system and allow further *in vivo* analysis to study human diseases, test new drugs or therapies many of which already have been examined in detail[85,143,181]. These mice are immunodeficient caused by mutations in the IL-2 receptor common γ-chain locus, which leads to functional impairment of immune cells like B, T and NK cells. Through intrahepatic injection of human $CD34^+$ hematopoietic stem cells a human immune system can be generated[141].

In the flow cytometry analysis of the included mice, human CD45 cells varied between 0.015% and 82% and the absolute number of $CD4^+$ T cells was determined, which was on average 41 cells/µL, so that the establishment of a humanized mouse model was successful. However, whether $CD4^+$ T cell count is critical to successful HIV-1 infection has not been investigated and needs to be determined. Furthermore, there are now many new approaches that improve the establishment of human immunity in mice. To this aim, it might be helpful to gather more

information about the sex, the method of stem cell injection, number of HSC[182]. The further evaluation of antibody-based therapy or CAR T cells in HIV-1 infected humanized mice is beyond this doctoral thesis.

6.3 scFvs as a suitable Candidate for the Target Domain

First trials using CD4 based CARs in HIV-1 infected individuals showed no significant reduction of viremia due to limited expansion and proliferation[130,183]. These first-generation HIV-1 specific T cells consisting out of the extracellular domain CD4 followed by an intracellular TCR derived CD3ζ chain was safe, but further investigation was required[170]. A few years later, second generation CD4-CARs were developed by several groups and cytolytic activity could be observed[184]. But there are some disadvantages in developing CD4 based CAR T cells. On the one hand, CD4-CARs could be outcompeted by native $CD4^+$ cells while binding to the HIV envelope protein and on the other hand, CD4 based CAR T cells might be susceptible to HIV infection[185]. Liu et al. generated a bispecific CAR T cell combining a CD4 and bNAb moiety and compared it to a monospecific CD4-CAR. Results showed enhanced antiviral activity and absence of viral entry[87,132]. In order to reduce the risk of CAR T cells being infected, gene editing tools like CRISPR/Cas9 have been used to generate HIV-resistant CAR T cells, which might be another effective strategy to develop anti-HIV CAR T cells[70,186].

Broadly neutralizing antibodies offer an alternative for generation of anti-HIV CAR T cells. But to target a high number of HIV strains and to evade escape mechanisms, a combination of CARs based on different bNAbs might be required[91,187]. This was confirmed in a clinical study in which two different bNAbs 3BNC117 and 10-1074 were combined and an antiviral effect could be achieved in viremic patients[84]. However, classic CAR T cells carry only one scFv on their cell surface. To evade antigen escape, tandem CARs or bispecific binding domains, as well as a combination of two different CARs should be developed but these have already been investigated by some groups[71,86,188].

In addition, several publications could show that produced single chain antibodies often tend to shape dimers or even multimers in solution[174,189]. This might be one reason why scFvs are less potent than IgGs. This could be possibly important for the generation of CAR T cells since aggregation of scFvs in a CAR construct could lead to loss of specificity and off target toxicity.

In recent years CAR technology has made an enormous progress. But more standardized assessments of CAR T cells are necessary, and it remains to be determined which CAR constructs are leading to an efficient activation and proliferation. Furthermore, additional data are required to clarify which variables are critical for CAR expression, transduction, and efficiency. Nevertheless, results already suggested that multiple co-stimulation domains

improve T cell effector functions[190]. Both *in vitro* and *in vivo* experiments indicated that in application of CD19 CAR T cells, the 4-1BB co-stimulatory domain was superior to CD28. A longer *in vivo* persistence and less T cell exhaustion could be achieved[110,191].
It might also be necessary to compare different CAR T cell constructs regarding their *in vitro* and *in vivo* behavior. The use of second and third generation CARs in clinical studies showed enhanced expansion of infused CAR T cells, improved progression free survival and safety in patients with hematological malignancies[121,126].
Thus, to fully investigate the potential efficacy of HIV-1 bNAb-derived CAR T cells, analysis in the context of the fully assembled CAR on the cellular surface will be required.

In summary, scFvs based on broadly neutralizing antibodies are in general a suitable candidate for the target domain of CARs against HIV-1. The investigated antibodies are less potent compared to full-length IgGs, however the difference is not so huge for all antibody classes, e.g., PGT145 and 1-79. However, the basic properties of IgGs are retained. The observations showed reduced stability of scFvs and reduced affinity towards their antigens. West et al. considered the geometry of scFvs including the linker region and antigen binding site as a reason for weaker binding[174,192]. Whereas, this might not be important for the generation of CAR T cells, as the antigen specificity will be enhanced by T cell effector functions. In addition to that, the weaker neutralization activity observed for scFvs might not be the decisive criterion for CAR T cells, but rather the binding behavior. The information that has been collected about IgGs for years will help to provide more information about the properties of scFv in order to find suitable candidates for the binding domain. However, further experiments and studies are necessary to gain conclusive information about the effectiveness of this therapeutic approach. At last, a humanized mouse model was successfully established, but further information for the development of a standardized procedure needs to be collected.

7. Conclusion

With this thesis, the possible use of scFvs as the extracellular binding domain of anti-HIV CAR T cells was evaluated. In a systemic investigation different anti-HIV bNAbs and their scFv derivatives were evaluated regarding reactivity, activity, and specificity.

In summary, the results showed comparable properties of scFvs to their full-length IgGs. We showed that scFvs bind to soluble and cell surface expressed envelope protein and that scFvs were able to neutralize a few HIV-1 pseudoviruses, although they obtained higher $IC_{50/80}$ values compared to the respective full-lengths antibodies. Two antibodies were found to make an exception: 1-79 and PGT145. Those scFvs were able to show comparable neutralization and binding behavior as the respective IgG1 and IgG4 antibody, making them possible candidates as a bNAb-based binding domain for the generation of anti-HIV-1 CAR T cells, since neutralization may not be as crucial for the CAR T cell design, compared to the well-binding of the antibodies. Furthermore, we could not observe an increase in auto-reactive properties of generated scFvs. Eventually, we were able to show that the scFv constructs showed a longer half-life in non-humanized mice compared to the IgG1 antibodies. These investigations might be valuable for design of CAR T cells. However, further investigations and construction of bNAb-based CAR T cells are required for a final statement.

At last, a humanized mouse model was successfully established, which is crucial for gaining more information about new therapy approaches. However, it is necessary to collect further knowledge to form a standardized procedure and increase the humanization efficiency.

8. References

1. Barre-Sinoussi F, Chermann JC, Rey F, et al. Isolation of a T-lymphotropic retrovirus from a patient at risk for acquired immune deficiency syndrome (AIDS). *Science* 1983; **220**(4599): 868-71.
2. Sharp PM, Hahn BH. Origins of HIV and the AIDS pandemic. *Cold Spring Harb Perspect Med* 2011; **1**(1): a006841.
3. Gallo RC, Salahuddin SZ, Popovic M, et al. Frequent detection and isolation of cytopathic retroviruses (HTLV-III) from patients with AIDS and at risk for AIDS. *Science* 1984; **224**(4648): 500-3.
4. Popovic M, Sarngadharan MG, Read E, Gallo RC. Detection, isolation, and continuous production of cytopathic retroviruses (HTLV-III) from patients with AIDS and pre-AIDS. *Science* 1984; **224**(4648): 497-500.
5. Gurgo C, Gallo RC. Human retroviruses: HTLV-I, II, and III and their association with leukemia and AIDS. *Ann N Y Acad Sci* 1987; **511**: 350-69.
6. Hahn BH, Shaw GM, De Cock KM, Sharp PM. AIDS as a zoonosis: scientific and public health implications. *Science* 2000; **287**(5453): 607-14.
7. Heeney JL, Rutjens E, Verschoor EJ, et al. Transmission of simian immunodeficiency virus SIVcpz and the evolution of infection in the presence and absence of concurrent human immunodeficiency virus type 1 infection in chimpanzees. *J Virol* 2006; **80**(14): 7208-18.
8. Huet T, Cheynier R, Meyerhans A, Roelants G, Wain-Hobson S. Genetic organization of a chimpanzee lentivirus related to HIV-1. *Nature* 1990; **345**(6273): 356-9.
9. Hirsch VM, Olmsted RA, Murphey-Corb M, Purcell RH, Johnson PR. An African primate lentivirus (SIVsm) closely related to HIV-2. *Nature* 1989; **339**(6223): 389-92.
10. Maartens G, Celum C, Lewin SR. HIV infection: epidemiology, pathogenesis, treatment, and prevention. *Lancet* 2014; **384**(9939): 258-71.
11. Merson MH, O'Malley J, Serwadda D, Apisuk C. The history and challenge of HIV prevention. *Lancet* 2008; **372**(9637): 475-88.
12. Worobey M, Gemmel M, Teuwen DE, et al. Direct evidence of extensive diversity of HIV-1 in Kinshasa by 1960. *Nature* 2008; **455**(7213): 661-4.
13. Taylor BS, Sobieszczyk ME, McCutchan FE, Hammer SM. The challenge of HIV-1 subtype diversity. *N Engl J Med* 2008; **358**(15): 1590-602.
14. Hemelaar J, Gouws E, Ghys PD, Osmanov S, Isolation W-UNfH, Characterisation. Global trends in molecular epidemiology of HIV-1 during 2000-2007. *AIDS* 2011; **25**(5): 679-89.
15. UNAIDS. HIV and AIDS Estimates, Germany. 2018. https://www.unaids.org/en/regionscountries/countries/germany (accessed 03.11.23 2023).
16. WHO. The top 10 causes of death. 09.12.2020 2020. https://www.who.int/news-room/fact-sheets/detail/the-top-10-causes-of-death (accessed 03.11.2023.
17. WHO. Antiretroviral therapy coverage estimates by WHO region. 20.07.2022 2022. https://apps.who.int/gho/data/view.main.23300REGION?lang=en (accessed 03.11.2023 2023).
18. Arts EJ, Hazuda DJ. HIV-1 antiretroviral drug therapy. *Cold Spring Harb Perspect Med* 2012; **2**(4): a007161.
19. Piot P, Laga M. Prostitutes: a high risk group for HIV infection? *Soz Praventivmed* 1988; **33**(7): 336-9.
20. Ngugi EN, Plummer FA, Simonsen JN, et al. Prevention of transmission of human immunodeficiency virus in Africa: effectiveness of condom promotion and health education among prostitutes. *Lancet* 1988; **2**(8616): 887-90.
21. Degenhardt L, Mathers B, Vickerman P, Rhodes T, Latkin C, Hickman M. Prevention of HIV infection for people who inject drugs: why individual, structural, and combination approaches are needed. *Lancet* 2010; **376**(9737): 285-301.
22. Beyrer C, Sullivan P, Sanchez J, et al. The increase in global HIV epidemics in MSM. *AIDS* 2013; **27**(17): 2665-78.

23. Antiretroviral Therapy Cohort C. Causes of death in HIV-1-infected patients treated with antiretroviral therapy, 1996-2006: collaborative analysis of 13 HIV cohort studies. *Clin Infect Dis* 2010; **50**(10): 1387-96.
24. Sonnenberg P, Glynn JR, Fielding K, Murray J, Godfrey-Faussett P, Shearer S. How soon after infection with HIV does the risk of tuberculosis start to increase? A retrospective cohort study in South African gold miners. *J Infect Dis* 2005; **191**(2): 150-8.
25. Cohen MS, Shaw GM, McMichael AJ, Haynes BF. Acute HIV-1 Infection. *N Engl J Med* 2011; **364**(20): 1943-54.
26. Shaw GM, Hunter E. HIV transmission. *Cold Spring Harb Perspect Med* 2012; **2**(11).
27. Haase AT. Targeting early infection to prevent HIV-1 mucosal transmission. *Nature* 2010; **464**(7286): 217-23.
28. Hufert FT, van Lunzen J, Janossy G, et al. Germinal centre CD4+ T cells are an important site of HIV replication in vivo. *AIDS* 1997; **11**(7): 849-57.
29. Tebit DM, Ndembi N, Weinberg A, Quinones-Mateu ME. Mucosal transmission of human immunodeficiency virus. *Curr HIV Res* 2012; **10**(1): 3-8.
30. Arthos J, Cicala C, Martinelli E, et al. HIV-1 envelope protein binds to and signals through integrin alpha4beta7, the gut mucosal homing receptor for peripheral T cells. *Nat Immunol* 2008; **9**(3): 301-9.
31. Walker B, McMichael A. The T-cell response to HIV. *Cold Spring Harb Perspect Med* 2012; **2**(11).
32. Shaik MM, Peng H, Lu J, et al. Structural basis of coreceptor recognition by HIV-1 envelope spike. *Nature* 2019; **565**(7739): 318-23.
33. Brenchley JM, Schacker TW, Ruff LE, et al. CD4+ T cell depletion during all stages of HIV disease occurs predominantly in the gastrointestinal tract. *J Exp Med* 2004; **200**(6): 749-59.
34. Veazey RS, DeMaria M, Chalifoux LV, et al. Gastrointestinal tract as a major site of CD4+ T cell depletion and viral replication in SIV infection. *Science* 1998; **280**(5362): 427-31.
35. Anton PA, Elliott J, Poles MA, et al. Enhanced levels of functional HIV-1 co-receptors on human mucosal T cells demonstrated using intestinal biopsy tissue. *AIDS* 2000; **14**(12): 1761-5.
36. Berger EA, Murphy PM, Farber JM. Chemokine receptors as HIV-1 coreceptors: roles in viral entry, tropism, and disease. *Annu Rev Immunol* 1999; **17**: 657-700.
37. Vanhamel J, Bruggemans A, Debyser Z. Establishment of latent HIV-1 reservoirs: what do we really know? *J Virus Erad* 2019; **5**(1): 3-9.
38. Siliciano JD, Kajdas J, Finzi D, et al. Long-term follow-up studies confirm the stability of the latent reservoir for HIV-1 in resting CD4+ T cells. *Nat Med* 2003; **9**(6): 727-8.
39. Chun TW, Stuyver L, Mizell SB, et al. Presence of an inducible HIV-1 latent reservoir during highly active antiretroviral therapy. *Proc Natl Acad Sci U S A* 1997; **94**(24): 13193-7.
40. Stein J, Storcksdieck Genannt Bonsmann M, Streeck H. Barriers to HIV Cure. *HLA* 2016; **88**(4): 155-63.
41. Persaud D, Gay H, Ziemniak C, et al. Absence of detectable HIV-1 viremia after treatment cessation in an infant. *N Engl J Med* 2013; **369**(19): 1828-35.
42. Richman DD, Margolis DM, Delaney M, Greene WC, Hazuda D, Pomerantz RJ. The challenge of finding a cure for HIV infection. *Science* 2009; **323**(5919): 1304-7.
43. Sadowski I, Hashemi FB. Strategies to eradicate HIV from infected patients: elimination of latent provirus reservoirs. *Cell Mol Life Sci* 2019; **76**(18): 3583-600.
44. Sgarbanti M, Battistini A. Therapeutics for HIV-1 reactivation from latency. *Curr Opin Virol* 2013; **3**(4): 394-401.
45. Bangham CR. CTL quality and the control of human retroviral infections. *Eur J Immunol* 2009; **39**(7): 1700-12.
46. Blanden RV. T cell response to viral and bacterial infection. *Transplant Rev* 1974; **19**(0): 56-88.
47. Goonetilleke N, Liu MK, Salazar-Gonzalez JF, et al. The first T cell response to transmitted/founder virus contributes to the control of acute viremia in HIV-1 infection. *J Exp Med* 2009; **206**(6): 1253-72.

48. Huang X, Chen H, Li W, et al. Precise determination of time to reach viral load set point after acute HIV-1 infection. *J Acquir Immune Defic Syndr* 2012; **61**(4): 448-54.
49. Shan L, Deng K, Shroff NS, et al. Stimulation of HIV-1-specific cytolytic T lymphocytes facilitates elimination of latent viral reservoir after virus reactivation. *Immunity* 2012; **36**(3): 491-501.
50. Deng K, Pertea M, Rongvaux A, et al. Broad CTL response is required to clear latent HIV-1 due to dominance of escape mutations. *Nature* 2015; **517**(7534): 381-5.
51. Schmitz JE, Kuroda MJ, Santra S, et al. Control of viremia in simian immunodeficiency virus infection by CD8+ lymphocytes. *Science* 1999; **283**(5403): 857-60.
52. Phillips RE, Rowland-Jones S, Nixon DF, et al. Human immunodeficiency virus genetic variation that can escape cytotoxic T cell recognition. *Nature* 1991; **354**(6353): 453-9.
53. Jones RB, Walker BD. HIV-specific CD8(+) T cells and HIV eradication. *J Clin Invest* 2016; **126**(2): 455-63.
54. Kerkau T, Schmitt-Landgraf R, Schimpl A, Wecker E. Downregulation of HLA class I antigens in HIV-1-infected cells. *AIDS Res Hum Retroviruses* 1989; **5**(6): 613-20.
55. Bodmer WF. The HLA system: structure and function. *J Clin Pathol* 1987; **40**(9): 948-58.
56. Collins DR, Gaiha GD, Walker BD. CD8(+) T cells in HIV control, cure and prevention. *Nat Rev Immunol* 2020; **20**(8): 471-82.
57. Allen TM, O'Connor DH, Jing P, et al. Tat-specific cytotoxic T lymphocytes select for SIV escape variants during resolution of primary viraemia. *Nature* 2000; **407**(6802): 386-90.
58. Day CL, Kaufmann DE, Kiepiela P, et al. PD-1 expression on HIV-specific T cells is associated with T-cell exhaustion and disease progression. *Nature* 2006; **443**(7109): 350-4.
59. Gaiha GD, McKim KJ, Woods M, et al. Dysfunctional HIV-specific CD8+ T cell proliferation is associated with increased caspase-8 activity and mediated by necroptosis. *Immunity* 2014; **41**(6): 1001-12.
60. West AP, Jr., Scharf L, Scheid JF, Klein F, Bjorkman PJ, Nussenzweig MC. Structural insights on the role of antibodies in HIV-1 vaccine and therapy. *Cell* 2014; **156**(4): 633-48.
61. Liu J, Bartesaghi A, Borgnia MJ, Sapiro G, Subramaniam S. Molecular architecture of native HIV-1 gp120 trimers. *Nature* 2008; **455**(7209): 109-13.
62. Tomaras GD, Yates NL, Liu P, et al. Initial B-cell responses to transmitted human immunodeficiency virus type 1: virion-binding immunoglobulin M (IgM) and IgG antibodies followed by plasma anti-gp41 antibodies with ineffective control of initial viremia. *J Virol* 2008; **82**(24): 12449-63.
63. Scanlan CN, Offer J, Zitzmann N, Dwek RA. Exploiting the defensive sugars of HIV-1 for drug and vaccine design. *Nature* 2007; **446**(7139): 1038-45.
64. Wibmer CK, Moore PL, Morris L. HIV broadly neutralizing antibody targets. *Curr Opin HIV AIDS* 2015; **10**(3): 135-43.
65. Lehmann C, Malin J, Suarez I, Fatkenheuer G. [Modern HIV treatment]. *Internist (Berl)* 2019; **60**(4): 411-9.
66. Liu B, Zhang W, Zhang H. Development of CAR-T cells for long-term eradication and surveillance of HIV-1 reservoir. *Curr Opin Virol* 2019; **38**: 21-30.
67. Kanters S, Vitoria M, Doherty M, et al. Comparative efficacy and safety of first-line antiretroviral therapy for the treatment of HIV infection: a systematic review and network meta-analysis. *Lancet HIV* 2016; **3**(11): e510-e20.
68. Llibre JM, Hung CC, Brinson C, et al. Efficacy, safety, and tolerability of dolutegravir-rilpivirine for the maintenance of virological suppression in adults with HIV-1: phase 3, randomised, non-inferiority SWORD-1 and SWORD-2 studies. *Lancet* 2018; **391**(10123): 839-49.
69. Ho YC, Shan L, Hosmane NN, et al. Replication-competent noninduced proviruses in the latent reservoir increase barrier to HIV-1 cure. *Cell* 2013; **155**(3): 540-51.
70. Hale M, Mesojednik T, Romano Ibarra GS, et al. Engineering HIV-Resistant, Anti-HIV Chimeric Antigen Receptor T Cells. *Mol Ther* 2017; **25**(3): 570-9.
71. Herzig E, Kim KC, Packard TA, et al. Attacking Latent HIV with convertibleCAR-T Cells, a Highly Adaptable Killing Platform. *Cell* 2019; **179**(4): 880-94 e10.

72. Weiss RA, Clapham PR, Cheingsong-Popov R, et al. Neutralization of human T-lymphotropic virus type III by sera of AIDS and AIDS-risk patients. *Nature* 1985; **316**(6023): 69-72.
73. Burton DR, Pyati J, Koduri R, et al. Efficient neutralization of primary isolates of HIV-1 by a recombinant human monoclonal antibody. *Science* 1994; **266**(5187): 1024-7.
74. McCoy LE. The expanding array of HIV broadly neutralizing antibodies. *Retrovirology* 2018; **15**(1): 70.
75. Simek MD, Rida W, Priddy FH, et al. Human immunodeficiency virus type 1 elite neutralizers: individuals with broad and potent neutralizing activity identified by using a high-throughput neutralization assay together with an analytical selection algorithm. *J Virol* 2009; **83**(14): 7337-48.
76. Halper-Stromberg A, Nussenzweig MC. Towards HIV-1 remission: potential roles for broadly neutralizing antibodies. *J Clin Invest* 2016; **126**(2): 415-23.
77. Wu X, Yang ZY, Li Y, et al. Rational design of envelope identifies broadly neutralizing human monoclonal antibodies to HIV-1. *Science* 2010; **329**(5993): 856-61.
78. Walker LM, Huber M, Doores KJ, et al. Broad neutralization coverage of HIV by multiple highly potent antibodies. *Nature* 2011; **477**(7365): 466-70.
79. Scheid JF, Mouquet H, Feldhahn N, et al. Broad diversity of neutralizing antibodies isolated from memory B cells in HIV-infected individuals. *Nature* 2009; **458**(7238): 636-40.
80. Overbaugh J, Morris L. The Antibody Response against HIV-1. *Cold Spring Harb Perspect Med* 2012; **2**(1): a007039.
81. Wei X, Decker JM, Wang S, et al. Antibody neutralization and escape by HIV-1. *Nature* 2003; **422**(6929): 307-12.
82. Mouquet H, Nussenzweig MC. Polyreactive antibodies in adaptive immune responses to viruses. *Cell Mol Life Sci* 2012; **69**(9): 1435-45.
83. Sather DN, Armann J, Ching LK, et al. Factors associated with the development of cross-reactive neutralizing antibodies during human immunodeficiency virus type 1 infection. *J Virol* 2009; **83**(2): 757-69.
84. Bar-On Y, Gruell H, Schoofs T, et al. Safety and antiviral activity of combination HIV-1 broadly neutralizing antibodies in viremic individuals. *Nat Med* 2018; **24**(11): 1701-7.
85. Klein F, Halper-Stromberg A, Horwitz JA, et al. HIV therapy by a combination of broadly neutralizing antibodies in humanized mice. *Nature* 2012; **492**(7427): 118-22.
86. Anthony-Gonda K, Bardhi A, Ray A, et al. Multispecific anti-HIV duoCAR-T cells display broad in vitro antiviral activity and potent in vivo elimination of HIV-infected cells in a humanized mouse model. *Sci Transl Med* 2019; **11**(504).
87. Liu L, Patel B, Ghanem MH, et al. Novel CD4-Based Bispecific Chimeric Antigen Receptor Designed for Enhanced Anti-HIV Potency and Absence of HIV Entry Receptor Activity. *J Virol* 2015; **89**(13): 6685-94.
88. Poignard P, Sabbe R, Picchio GR, et al. Neutralizing antibodies have limited effects on the control of established HIV-1 infection in vivo. *Immunity* 1999; **10**(4): 431-8.
89. Hessell AJ, Poignard P, Hunter M, et al. Effective, low-titer antibody protection against low-dose repeated mucosal SHIV challenge in macaques. *Nat Med* 2009; **15**(8): 951-4.
90. Mendoza P, Gruell H, Nogueira L, et al. Combination therapy with anti-HIV-1 antibodies maintains viral suppression. *Nature* 2018; **561**(7724): 479-84.
91. Caskey M, Schoofs T, Gruell H, et al. Antibody 10-1074 suppresses viremia in HIV-1-infected individuals. *Nat Med* 2017.
92. Caskey M, Klein F, Lorenzi JC, et al. Viraemia suppressed in HIV-1-infected humans by broadly neutralizing antibody 3BNC117. *Nature* 2015; **522**(7557): 487-91.
93. Kumar R, Qureshi H, Deshpande S, Bhattacharya J. Broadly neutralizing antibodies in HIV-1 treatment and prevention. *Ther Adv Vaccines Immunother* 2018; **6**(4): 61-8.
94. Gruell H, Klein F. Antibody-mediated prevention and treatment of HIV-1 infection. *Retrovirology* 2018; **15**(1): 73.
95. Borducchi EN, Liu J, Nkolola JP, et al. Antibody and TLR7 agonist delay viral rebound in SHIV-infected monkeys. *Nature* 2018; **563**(7731): 360-4.
96. Cohen YZ, Lorenzi JCC, Krassnig L, et al. Relationship between latent and rebound viruses in a clinical trial of anti-HIV-1 antibody 3BNC117. *J Exp Med* 2018; **215**(9): 2311-24.

97. Gruell H, Gunst JD, Cohen YZ, et al. Effect of 3BNC117 and romidepsin on the HIV-1 reservoir in people taking suppressive antiretroviral therapy (ROADMAP): a randomised, open-label, phase 2A trial. *Lancet Microbe* 2022; **3**(3): e203-e14.
98. Walker BD, Chakrabarti S, Moss B, et al. HIV-specific cytotoxic T lymphocytes in seropositive individuals. *Nature* 1987; **328**(6128): 345-8.
99. Cheadle EJ, Sheard V, Hombach AA, et al. Chimeric antigen receptors for T-cell based therapy. *Methods Mol Biol* 2012; **907**: 645-66.
100. Kochenderfer JN, Dudley ME, Feldman SA, et al. B-cell depletion and remissions of malignancy along with cytokine-associated toxicity in a clinical trial of anti-CD19 chimeric-antigen-receptor-transduced T cells. *Blood* 2012; **119**(12): 2709-20.
101. Uckun FM, Jaszcz W, Ambrus JL, et al. Detailed studies on expression and function of CD19 surface determinant by using B43 monoclonal antibody and the clinical potential of anti-CD19 immunotoxins. *Blood* 1988; **71**(1): 13-29.
102. Porter DL, Levine BL, Kalos M, Bagg A, June CH. Chimeric antigen receptor-modified T cells in chronic lymphoid leukemia. *N Engl J Med* 2011; **365**(8): 725-33.
103. Grupp SA, Kalos M, Barrett D, et al. Chimeric antigen receptor-modified T cells for acute lymphoid leukemia. *N Engl J Med* 2013; **368**(16): 1509-18.
104. Geyer MB. First CAR to Pass the Road Test: Tisagenlecleucel's Drive to FDA Approval. *Clin Cancer Res* 2019; **25**(4): 1133-5.
105. Liu B, Zhang W, Xia B, et al. Broadly neutralizing antibody-derived CAR T cells reduce viral reservoir in individuals infected with HIV-1. *J Clin Invest* 2021; **131**(19).
106. Alarcon B, Gil D, Delgado P, Schamel WW. Initiation of TCR signaling: regulation within CD3 dimers. *Immunol Rev* 2003; **191**: 38-46.
107. Mariuzza RA, Agnihotri P, Orban J. The structural basis of T-cell receptor (TCR) activation: An enduring enigma. *J Biol Chem* 2020; **295**(4): 914-25.
108. Garcia KC, Degano M, Stanfield RL, et al. An alphabeta T cell receptor structure at 2.5 A and its orientation in the TCR-MHC complex. *Science* 1996; **274**(5285): 209-19.
109. Romeo C, Seed B. Cellular immunity to HIV activated by CD4 fused to T cell or Fc receptor polypeptides. *Cell* 1991; **64**(5): 1037-46.
110. Sadelain M, Brentjens R, Riviere I. The basic principles of chimeric antigen receptor design. *Cancer Discov* 2013; **3**(4): 388-98.
111. Ali A, Kitchen SG, Chen IS, Ng HL, Zack JA, Yang OO. HIV-1-Specific Chimeric Antigen Receptors Based on Broadly Neutralizing Antibodies. *J Virol* 2016; **90**(15): 6999-7006.
112. Jensen MC, Riddell SR. Design and implementation of adoptive therapy with chimeric antigen receptor-modified T cells. *Immunol Rev* 2014; **257**(1): 127-44.
113. Eshhar Z, Waks T, Gross G, Schindler DG. Specific activation and targeting of cytotoxic lymphocytes through chimeric single chains consisting of antibody-binding domains and the gamma or zeta subunits of the immunoglobulin and T-cell receptors. *Proc Natl Acad Sci U S A* 1993; **90**(2): 720-4.
114. June CH, Levine BL. T cell engineering as therapy for cancer and HIV: our synthetic future. *Philos Trans R Soc Lond B Biol Sci* 2015; **370**(1680): 20140374.
115. Aleksic M, Liddy N, Molloy PE, et al. Different affinity windows for virus and cancer-specific T-cell receptors: implications for therapeutic strategies. *Eur J Immunol* 2012; **42**(12): 3174-9.
116. Dotti G, Gottschalk S, Savoldo B, Brenner MK. Design and development of therapies using chimeric antigen receptor-expressing T cells. *Immunol Rev* 2014; **257**(1): 107-26.
117. Gill S, June CH. Going viral: chimeric antigen receptor T-cell therapy for hematological malignancies. *Immunol Rev* 2015; **263**(1): 68-89.
118. Schroeder HW, Jr., Cavacini L. Structure and function of immunoglobulins. *J Allergy Clin Immunol* 2010; **125**(2 Suppl 2): S41-52.
119. Jonnalagadda M, Mardiros A, Urak R, et al. Chimeric antigen receptors with mutated IgG4 Fc spacer avoid fc receptor binding and improve T cell persistence and antitumor efficacy. *Mol Ther* 2015; **23**(4): 757-68.
120. Hudecek M, Lupo-Stanghellini MT, Kosasih PL, et al. Receptor affinity and extracellular domain modifications affect tumor recognition by ROR1-specific chimeric antigen receptor T cells. *Clin Cancer Res* 2013; **19**(12): 3153-64.

121. Savoldo B, Ramos CA, Liu E, et al. CD28 costimulation improves expansion and persistence of chimeric antigen receptor-modified T cells in lymphoma patients. *J Clin Invest* 2011; **121**(5): 1822-6.
122. Gong MC, Latouche JB, Krause A, Heston WD, Bander NH, Sadelain M. Cancer patient T cells genetically targeted to prostate-specific membrane antigen specifically lyse prostate cancer cells and release cytokines in response to prostate-specific membrane antigen. *Neoplasia* 1999; **1**(2): 123-7.
123. Kowolik CM, Topp MS, Gonzalez S, et al. CD28 costimulation provided through a CD19-specific chimeric antigen receptor enhances in vivo persistence and antitumor efficacy of adoptively transferred T cells. *Cancer Res* 2006; **66**(22): 10995-1004.
124. Milone MC, Fish JD, Carpenito C, et al. Chimeric receptors containing CD137 signal transduction domains mediate enhanced survival of T cells and increased antileukemic efficacy in vivo. *Mol Ther* 2009; **17**(8): 1453-64.
125. Cheng Z, Wei R, Ma Q, et al. In Vivo Expansion and Antitumor Activity of Coinfused CD28- and 4-1BB-Engineered CAR-T Cells in Patients with B Cell Leukemia. *Mol Ther* 2018; **26**(4): 976-85.
126. Till BG, Jensen MC, Wang J, et al. CD20-specific adoptive immunotherapy for lymphoma using a chimeric antigen receptor with both CD28 and 4-1BB domains: pilot clinical trial results. *Blood* 2012; **119**(17): 3940-50.
127. Zhong XS, Matsushita M, Plotkin J, Riviere I, Sadelain M. Chimeric antigen receptors combining 4-1BB and CD28 signaling domains augment PI3kinase/AKT/Bcl-XL activation and CD8+ T cell-mediated tumor eradication. *Mol Ther* 2010; **18**(2): 413-20.
128. Cooper LJ, Kalos M, Lewinsohn DA, Riddell SR, Greenberg PD. Transfer of specificity for human immunodeficiency virus type 1 into primary human T lymphocytes by introduction of T-cell receptor genes. *J Virol* 2000; **74**(17): 8207-12.
129. Kuhlmann AS, Peterson CW, Kiem HP. Chimeric antigen receptor T-cell approaches to HIV cure. *Curr Opin HIV AIDS* 2018; **13**(5): 446-53.
130. Deeks SG, Wagner B, Anton PA, et al. A phase II randomized study of HIV-specific T-cell gene therapy in subjects with undetectable plasma viremia on combination antiretroviral therapy. *Mol Ther* 2002; **5**(6): 788-97.
131. Morgan RA, Yang JC, Kitano M, Dudley ME, Laurencot CM, Rosenberg SA. Case report of a serious adverse event following the administration of T cells transduced with a chimeric antigen receptor recognizing ERBB2. *Mol Ther* 2010; **18**(4): 843-51.
132. Campos-Gonzalez G, Martinez-Picado J, Velasco-Hernandez T, Salgado M. Opportunities for CAR-T Cell Immunotherapy in HIV Cure. *Viruses* 2023; **15**(3).
133. Maus MV, Fraietta JA, Levine BL, Kalos M, Zhao Y, June CH. Adoptive immunotherapy for cancer or viruses. *Annu Rev Immunol* 2014; **32**: 189-225.
134. Maude SL, Frey N, Shaw PA, et al. Chimeric antigen receptor T cells for sustained remissions in leukemia. *N Engl J Med* 2014; **371**(16): 1507-17.
135. Sautto GA, Wisskirchen K, Clementi N, et al. Chimeric antigen receptor (CAR)-engineered T cells redirected against hepatitis C virus (HCV) E2 glycoprotein. *Gut* 2016; **65**(3): 512-23.
136. Sun S, Hao H, Yang G, Zhang Y, Fu Y. Immunotherapy with CAR-Modified T Cells: Toxicities and Overcoming Strategies. *J Immunol Res* 2018; **2018**: 2386187.
137. Hay KA. Cytokine release syndrome and neurotoxicity after CD19 chimeric antigen receptor-modified (CAR-) T cell therapy. *Br J Haematol* 2018; **183**(3): 364-74.
138. Khadka RH, Sakemura R, Kenderian SS, Johnson AJ. Management of cytokine release syndrome: an update on emerging antigen-specific T cell engaging immunotherapies. *Immunotherapy* 2019; **11**(10): 851-7.
139. Wang X, Chang WC, Wong CW, et al. A transgene-encoded cell surface polypeptide for selection, in vivo tracking, and ablation of engineered cells. *Blood* 2011; **118**(5): 1255-63.
140. Lee DW, Gardner R, Porter DL, et al. Current concepts in the diagnosis and management of cytokine release syndrome. *Blood* 2014; **124**(2): 188-95.
141. Shultz LD, Brehm MA, Garcia-Martinez JV, Greiner DL. Humanized mice for immune system investigation: progress, promise and challenges. *Nat Rev Immunol* 2012; **12**(11): 786-98.

142. Weichseldorfer M, Heredia A, Reitz M, Bryant JL, Latinovic OS. Use of Humanized Mouse Models for Studying HIV-1 Infection, Pathogenesis and Persistence. *J AIDS HIV Treat* 2020; **2**(1): 23-9.
143. Masse-Ranson G, Mouquet H, Di Santo JP. Humanized mouse models to study pathophysiology and treatment of HIV infection. *Curr Opin HIV AIDS* 2018; **13**(2): 143-51.
144. Schommers P, Gruell H, Abernathy ME, et al. Restriction of HIV-1 Escape by a Highly Broad and Potent Neutralizing Antibody. *Cell* 2020; **180**(3): 471-89 e22.
145. Platt EJ, Wehrly K, Kuhmann SE, Chesebro B, Kabat D. Effects of CCR5 and CD4 cell surface concentrations on infections by macrophagetropic isolates of human immunodeficiency virus type 1. *J Virol* 1998; **72**(4): 2855-64.
146. Kilkenny C, Browne WJ, Cuthill IC, Emerson M, Altman DG. Improving bioscience research reporting: the ARRIVE guidelines for reporting animal research. *Osteoarthritis Cartilage* 2012; **20**(4): 256-60.
147. Hombach A, Koch D, Sircar R, et al. A chimeric receptor that selectively targets membrane-bound carcinoembryonic antigen (mCEA) in the presence of soluble CEA. *Gene Ther* 1999; **6**(2): 300-4.
148. Wardemann H, Yurasov S, Schaefer A, Young JW, Meffre E, Nussenzweig MC. Predominant autoantibody production by early human B cell precursors. *Science* 2003; **301**(5638): 1374-7.
149. Silva JP, Vetterlein O, Jose J, Peters S, Kirby H. The S228P mutation prevents in vivo and in vitro IgG4 Fab-arm exchange as demonstrated using a combination of novel quantitative immunoassays and physiological matrix preparation. *J Biol Chem* 2015; **290**(9): 5462-9.
150. Pietzsch J, Scheid JF, Mouquet H, et al. Human anti-HIV-neutralizing antibodies frequently target a conserved epitope essential for viral fitness. *J Exp Med* 2010; **207**(9): 1995-2002.
151. Rajan A, Piedra FA, Aideyan L, et al. Multiple Respiratory Syncytial Virus (RSV) Strains Infecting HEp-2 and A549 Cells Reveal Cell Line-Dependent Differences in Resistance to RSV Infection. *J Virol* 2022; **96**(7): e0190421.
152. Tan EM, Rodnan GP, Garcia I, Moroi Y, Fritzler MJ, Peebles C. Diversity of antinuclear antibodies in progressive systemic sclerosis. Anti-centromere antibody and its relationship to CREST syndrome. *Arthritis Rheum* 1980; **23**(6): 617-25.
153. Moroi Y, Peebles C, Fritzler MJ, Steigerwald J, Tan EM. Autoantibody to centromere (kinetochore) in scleroderma sera. *Proc Natl Acad Sci U S A* 1980; **77**(3): 1627-31.
154. Sarzotti-Kelsoe M, Bailer RT, Turk E, et al. Optimization and validation of the TZM-bl assay for standardized assessments of neutralizing antibodies against HIV-1. *J Immunol Methods* 2014; **409**: 131-46.
155. Klein F, Gaebler C, Mouquet H, et al. Broad neutralization by a combination of antibodies recognizing the CD4 binding site and a new conformational epitope on the HIV-1 envelope protein. *J Exp Med* 2012; **209**(8): 1469-79.
156. Schoofs T, Barnes CO, Suh-Toma N, et al. Broad and Potent Neutralizing Antibodies Recognize the Silent Face of the HIV Envelope. *Immunity* 2019; **50**(6): 1513-29 e9.
157. Yoon H, Macke J, West AP, Jr., et al. CATNAP: a tool to compile, analyze and tally neutralizing antibody panels. *Nucleic Acids Res* 2015; **43**(W1): W213-9.
158. Yang X, Farzan M, Wyatt R, Sodroski J. Characterization of stable, soluble trimers containing complete ectodomains of human immunodeficiency virus type 1 envelope glycoproteins. *J Virol* 2000; **74**(12): 5716-25.
159. Scharf L, Wang H, Gao H, Chen S, McDowall AW, Bjorkman PJ. Broadly Neutralizing Antibody 8ANC195 Recognizes Closed and Open States of HIV-1 Env. *Cell* 2015; **162**(6): 1379-90.
160. Rujas E, Gulzar N, Morante K, et al. Structural and Thermodynamic Basis of Epitope Binding by Neutralizing and Nonneutralizing Forms of the Anti-HIV-1 Antibody 4E10. *J Virol* 2015; **89**(23): 11975-89.
161. Feng Y, McKee K, Tran K, et al. Biochemically defined HIV-1 envelope glycoprotein variant immunogens display differential binding and neutralizing specificities to the CD4-binding site. *J Biol Chem* 2012; **287**(8): 5673-86.

162. Mouquet H, Scheid JF, Zoller MJ, et al. Polyreactivity increases the apparent affinity of anti-HIV antibodies by heteroligation. *Nature* 2010; **467**(7315): 591-5.
163. Haynes BF, Fleming J, St Clair EW, et al. Cardiolipin polyspecific autoreactivity in two broadly neutralizing HIV-1 antibodies. *Science* 2005; **308**(5730): 1906-8.
164. Diskin R, Klein F, Horwitz JA, et al. Restricting HIV-1 pathways for escape using rationally designed anti-HIV-1 antibodies. *J Exp Med* 2013; **210**(6): 1235-49.
165. Stitz J, Steidl S, Merget-Millitzer H, et al. MLV-derived retroviral vectors selective for CD4-expressing cells and resistant to neutralization by sera from HIV-infected patients. *Virology* 2000; **267**(2): 229-36.
166. Schoofs T, Klein F, Braunschweig M, et al. HIV-1 therapy with monoclonal antibody 3BNC117 elicits host immune responses against HIV-1. *Science* 2016; **352**(6288): 997-1001.
167. Lee JH, Andrabi R, Su CY, et al. A Broadly Neutralizing Antibody Targets the Dynamic HIV Envelope Trimer Apex via a Long, Rigidified, and Anionic beta-Hairpin Structure. *Immunity* 2017; **46**(4): 690-702.
168. Prins JM, Jurriaans S, van Praag RM, et al. Immuno-activation with anti-CD3 and recombinant human IL-2 in HIV-1-infected patients on potent antiretroviral therapy. *AIDS* 1999; **13**(17): 2405-10.
169. Archin NM, Liberty AL, Kashuba AD, et al. Administration of vorinostat disrupts HIV-1 latency in patients on antiretroviral therapy. *Nature* 2012; **487**(7408): 482-5.
170. Walker RE, Bechtel CM, Natarajan V, et al. Long-term in vivo survival of receptor-modified syngeneic T cells in patients with human immunodeficiency virus infection. *Blood* 2000; **96**(2): 467-74.
171. Scholler J, Brady TL, Binder-Scholl G, et al. Decade-long safety and function of retroviral-modified chimeric antigen receptor T cells. *Sci Transl Med* 2012; **4**(132): 132ra53.
172. Holliger P, Hudson PJ. Engineered antibody fragments and the rise of single domains. *Nat Biotechnol* 2005; **23**(9): 1126-36.
173. Wang HW, Cole D, Jiang WZ, et al. Engineering and functional evaluation of a single-chain antibody against HIV-1 external glycoprotein gp120. *Clin Exp Immunol* 2005; **141**(1): 72-80.
174. West AP, Jr., Galimidi RP, Gnanapragasam PN, Bjorkman PJ. Single-chain Fv-based anti-HIV proteins: potential and limitations. *J Virol* 2012; **86**(1): 195-202.
175. Yu L, Guan Y. Immunologic Basis for Long HCDR3s in Broadly Neutralizing Antibodies Against HIV-1. *Front Immunol* 2014; **5**: 250.
176. Klein F, Nogueira L, Nishimura Y, et al. Enhanced HIV-1 immunotherapy by commonly arising antibodies that target virus escape variants. *J Exp Med* 2014; **211**(12): 2361-72.
177. Kwong PD, Wyatt R, Robinson J, Sweet RW, Sodroski J, Hendrickson WA. Structure of an HIV gp120 envelope glycoprotein in complex with the CD4 receptor and a neutralizing human antibody. *Nature* 1998; **393**(6686): 648-59.
178. Zolla-Pazner S, Cohen SS, Boyd D, et al. Structure/Function Studies Involving the V3 Region of the HIV-1 Envelope Delineate Multiple Factors That Affect Neutralization Sensitivity. *J Virol* 2016; **90**(2): 636-49.
179. Ong YT, Kirby KA, Hachiya A, et al. Preparation of biologically active single-chain variable antibody fragments that target the HIV-1 gp120 V3 loop. *Cell Mol Biol (Noisy-le-grand)* 2012; **58**(1): 71-9.
180. Maruta Y, Kuwata T, Tanaka K, et al. Cross-Neutralization Activity of Single-Chain Variable Fragment (scFv) Derived from Anti-V3 Monoclonal Antibodies Mediated by Post-Attachment Binding. *Jpn J Infect Dis* 2016; **69**(5): 395-404.
181. Zumwalde NA, Gumperz JE. Modeling Human Antitumor Responses In Vivo Using Umbilical Cord Blood-Engrafted Mice. *Front Immunol* 2018; **9**: 54.
182. Stripecke R, Munz C, Schuringa JJ, et al. Innovations, challenges, and minimal information for standardization of humanized mice. *EMBO Mol Med* 2020; **12**(7): e8662.
183. Zhen A, Peterson CW, Carrillo MA, et al. Long-term persistence and function of hematopoietic stem cell-derived chimeric antigen receptor T cells in a nonhuman primate model of HIV/AIDS. *PLoS Pathog* 2017; **13**(12): e1006753.

184. Sahu GK, Sango K, Selliah N, Ma Q, Skowron G, Junghans RP. Anti-HIV designer T cells progressively eradicate a latently infected cell line by sequentially inducing HIV reactivation then killing the newly gp120-positive cells. *Virology* 2013; **446**(1-2): 268-75.
185. Zhen A, Kamata M, Rezek V, et al. HIV-specific Immunity Derived From Chimeric Antigen Receptor-engineered Stem Cells. *Mol Ther* 2015; **23**(8): 1358-67.
186. Rothemejer FH, Lauritsen NP, Juhl AK, et al. Development of HIV-Resistant CAR T Cells by CRISPR/Cas-Mediated CAR Integration into the CCR5 Locus. *Viruses* 2023; **15**(1).
187. Wagner TA. Quarter Century of Anti-HIV CAR T Cells. *Curr HIV/AIDS Rep* 2018; **15**(2): 147-54.
188. Schneider D, Xiong Y, Wu D, et al. A tandem CD19/CD20 CAR lentiviral vector drives on-target and off-target antigen modulation in leukemia cell lines. *J Immunother Cancer* 2017; **5**: 42.
189. Wu Y, Jiang S, Ying T. From therapeutic antibodies to chimeric antigen receptors (CARs): making better CARs based on antigen-binding domain. *Expert Opin Biol Ther* 2016; **16**(12): 1469-78.
190. Liu B, Zou F, Lu L, et al. Chimeric Antigen Receptor T Cells Guided by the Single-Chain Fv of a Broadly Neutralizing Antibody Specifically and Effectively Eradicate Virus Reactivated from Latency in CD4+ T Lymphocytes Isolated from HIV-1-Infected Individuals Receiving Suppressive Combined Antiretroviral Therapy. *J Virol* 2016; **90**(21): 9712-24.
191. Long AH, Haso WM, Shern JF, et al. 4-1BB costimulation ameliorates T cell exhaustion induced by tonic signaling of chimeric antigen receptors. *Nat Med* 2015; **21**(6): 581-90.
192. Bird RE, Walker BW. Single chain antibody variable regions. *Trends Biotechnol* 1991; **9**(4): 132-7.

9. Appendix

9.1 List of Figures

Figure 1: Antibody binding sites on the HIV envelope protein. 16
Figure 2: Schematic representation of CAR and T cell receptor. 19
Figure 3: Humanization of NOD-Rag1^{null}IL2rg^{null} (NRG) mice. 32
Figure 4: Three different antibody classes. 34
Figure 5: Successful antibody expression confirmed by SDS PAGE. 35
Figure 6: Comparison of antibody concentrations of five different bNAbs. 36
Figure 7: Expression of eluted envelope protein YU2gp140 after purification with Ni-NTA beads. 37
Figure 8: Antibodies tested in an ELISA against soluble YU2$_{gp140.}$ 38
Figure 9: Binding between cell surface expressed YU2$_{gp140}$ and BaL$_{gp140}$ and antibodies. 39
Figure 10: Gating strategy for FACS analysis of NIH4546 IgG1 against BaL$_{gp140}$ (A-D) and overlay plot of NIH4546 against YU2$_{gp140}$ and BaL$_{gp140}$ (E, F). 40
Figure 11: Scale bars representing fold change of MFI normalized on NIH4546. 41
Figure 12: *In vivo* application of five antibody constructs in non-humanized mice. 42
Figure 13: Evaluation of the polyreactivity in a clinical validated HEp-2 cell assay. 45
Figure 14: FACS dot plot exemplary for a successfully humanized mouse. 49

9.2 List of Tables

Table 1: Materials and resources table 23
Table 2: Measured IC$_{50}$ and IC$_{80}$ values from TZM.bl assay. 47